

Photon elastic scattering simulation: validation and improvements to Geant4

Matej Batič, Gabriela Hoff, Maria Grazia Pia and Paolo Saracco

Abstract—Several models for the simulation of photon elastic scattering are quantitatively evaluated with respect to a large collection of experimental data retrieved from the literature. They include models based on the form factor approximation, on S-matrix calculations and on analytical parameterizations; they exploit publicly available data libraries and tabulations of theoretical calculations. Some of these models are currently implemented in general purpose Monte Carlo systems; some have been implemented and evaluated for the first time in this paper for possible use in Monte Carlo particle transport. The analysis mainly concerns the energy range between 5 keV and a few MeV. The validation process identifies the newly implemented model based on second order S-matrix calculations as the one best reproducing experimental measurements. The validation results show that, along with Rayleigh scattering, additional processes, not yet implemented in Geant4 nor in other major Monte Carlo systems, should be taken into account to realistically describe photon elastic scattering with matter above 1 MeV. Evaluations of the computational performance of the various simulation algorithms are reported along with the analysis of their physics capabilities.

Index Terms—Monte Carlo, simulation, Geant4, X-rays

I. INTRODUCTION

PHOTON elastic scattering is important in various experimental domains, such as material analysis applications, medical diagnostics and imaging [1]; more in general, elastic interactions contribute to the determination of photon mass attenuation coefficients, which are widely used parameters in medical physics and radiation protection [2]. In the energy range between approximately 1 keV and few MeV, which is the object of this paper, the resolution of modern detectors, high intensity synchrotron radiation sources and, in recent years, the availability of resources for large scale numerical computations have concurred to build a wide body of knowledge on photon elastic scattering. Extensive reviews of photon elastic scattering, that cover both its theoretical and experimental aspects, can be found in the literature (e.g. [3]–[5]).

This paper addresses this topic under a pragmatic perspective: its simulation in general purpose Monte Carlo codes

for particle transport. Photon interactions with matter, both elastic and inelastic, play a critical role in these systems; their modeling presents some peculiarities, because the software must satisfy concurrent requirements of physical accuracy and computational performance.

Photon-atom elastic scattering encompasses various interactions, but Rayleigh scattering, i.e. scattering from bound electrons, is the dominant contribution in the low energy régime and, as energy increases, remains dominant in a progressively smaller angular range of forward scattering. Rayleigh scattering models are implemented in all general-purpose Monte Carlo systems; comparison studies have highlighted discrepancies among some of them [6], nevertheless a comprehensive, quantitative appraisal of their validity is not yet documented in the literature. It is worthwhile to note that the validation of simulation models implies their comparison with experimental measurements [7]; comparisons with tabulations of theoretical calculations or analytical parameterizations, such as those that are reported in [8] as validation of Geant4 [9], [10] photon cross sections, do not constitute a validation of the simulation software.

This paper evaluates the models adopted by general-purpose Monte Carlo systems and other modeling approaches not yet implemented in these codes, to identify the state-of-the-art in the simulation of photon elastic scattering. Computational performance imposes constraints on the complexity of physics calculations to be performed in the course of simulation: hence the analysis is limited to theoretical models for which tabulations of pre-calculated values are available, or that are expressed by means of simple analytical formulations. To be relevant for general purpose Monte Carlo systems, tabulated data should cover the whole periodic table of elements and an extended energy range. The accuracy of elastic scattering simulation models is quantified with statistical methods comparing them with a wide collection of experimental data retrieved from the literature; the evaluation of physics capabilities is complemented by the estimate of their computational performance. These results provide guidance for the selection of physics models in simulation applications in response to the requirements of physics accuracy and computational speed pertinent to different experimental scenarios.

Special emphasis is devoted to the validation and possible improvement of photon elastic scattering modeling in Geant4; nevertheless, the results documented in this paper can be of more general interest also for other Monte Carlo systems.

Manuscript received 28 February 2012.

This work has been partly funded by CNPq BEX6460/10-0 grant, Brazil.

M. Batič is with INFN Sezione di Genova, Genova, Italy (e-mail: Matej.Batic@ge.infn.it); he is on leave from Jozef Stefan Institute, 1000 Ljubljana, Slovenia.

G. Hoff is with INFN Sezione di Genova, Genova, Italy (e-mail: Gabriela.Hoff@ge.infn.it); she is on leave from Pontificia Universidade Catolica do Rio Grande do Sul, Brazil.

M. G. Pia and Paolo Saracco are with INFN Sezione di Genova, Via Dodecaneso 33, I-16146 Genova, Italy (phone: +39 010 3536328, fax: +39 010 313358, MariaGrazia.Pia@ge.infn.it, Paolo.Saracco@ge.infn.it).

II. PHYSICS OVERVIEW

Photon-atom elastic scattering has been the object of theoretical and experimental interest for several decades; only a brief overview is summarized here to facilitate the comprehension of the software developments and simulation validation results documented in this paper.

Conventionally, photon-atom interactions are classified into elastic and inelastic processes, depending on whether the photon energy changes in the center of mass frame: although commonly applied in atomic physics practice and Monte Carlo transport, this distinction is somewhat arbitrary, since QED (quantum electrodynamics) radiative corrections and target recoil actually make all processes inelastic and, on the experimental side, the classification of a process as elastic or inelastic is limited by source bandwidth and detector resolution.

The physics models considered in this study concern isolated photon-atom scattering: they neglect the effects of the environment of the target atom and multi-photon effects associated with incident beams. They do not take into account either any internal degrees of freedom of the initial or final atom, such as its orientation; therefore they do not describe X-ray scattering from electrons in molecules and oriented solids. This scenario is consistent with the assumptions of general-purpose Monte Carlo systems for particle transport, where particles are assumed to interact with free atoms of the medium.

A. Theoretical calculations

Elastic photon-atom scattering encompasses various types of interactions, which are usually distinguished as:

- Rayleigh scattering, for scattering from the atomic electrons,
- nuclear Thomson scattering, for scattering from the nucleus considered as a point charge,
- Delbrück scattering, for scattering from the field of the nucleus,
- nuclear resonance scattering, for scattering from the internal structure of the nucleus.

These amplitudes are coherent, i.e. not physically distinguishable; the total elastic amplitude is commonly calculated as the sum of these separate amplitudes. There are still unresolved questions about the additivity of the amplitudes from composite systems, due to the complex interplay in a composite system between partitioning the total amplitude and the reduction from a many-body photon-atom interaction to an effective single particle formalism [11]; open issues concern the effects of electron correlations and of the finite lifetimes of atomic excited states [3].

Rayleigh scattering calculations are commonly performed by means of an approximation, that describes the scattering amplitude in terms of the form factor, which represents the Fourier transform of the charge density of the atom. This can be simply understood considering the two Thomson amplitudes from a free (point-like) particle [12]:

$$A_{||}^T = -r_0 \cos \theta, \quad A_{\perp}^T = -r_0 \quad (1)$$

leading to a differential cross section

$$\frac{d\sigma}{d\Omega} = \frac{r_0}{2} (1 + \cos^2 \theta) \quad (2)$$

which, for coherent scattering, is modified in presence of a charge distribution in

$$\frac{d\sigma}{d\Omega} = \frac{r_0}{2} (1 + \cos^2 \theta) F^2(q, Z) \quad (3)$$

where σ represents the cross section, Ω is the solid angle, r_0 is the classical electron radius, θ is the scattering angle, $F(q, Z)$ is the atomic form factor as a function of momentum transfer q and atomic number Z of the target atom. This approximation is valid for photon energies much greater than electron binding energies and for non-relativistic momentum transfers, which in this case is meant as $\hbar q \ll m_e c$, where \hbar is the reduced Planck constant, m_e is the electron mass and c is the speed of light. In the so-called ‘‘modified form factor’’ approximation each subshell charge density is multiplied by a different factor.

Various calculations of non-relativistic, relativistic and modified relativistic form factors are documented in the literature; the tabulations by Hubbell et al. [13], Hubbell and Øverbø [14], and Schaupp et al. [15], respectively of non-relativistic, relativistic and modified form factors, are representative of this approach.

For forward scattering the difference between the form factor amplitude and the exact amplitude is described by two anomalous scattering factors [3], that take into account the persistence of binding effects even in the high energy limit of Rayleigh scattering.

A more consistent approach for the description of elastic photon-atom scattering involves the evaluation of the relativistic second order S-matrix element in independent particle approximation. Relativistic quantum electrodynamics, treated in lowest non-vanishing order in e^2 , provides the basic theoretical framework for these calculations; neglect of higher order terms in e^2 in the calculation means that radiative corrections are not taken into account. The mass of the atomic nucleus is assumed to be infinite compared to the photon energy in question; therefore only scattering from atomic electrons is considered. This many-electron state is treated in a self-consistent central field approximation, in which each electron is assumed to move in an average potential due to all atomic electrons and the nucleus.

Numerical evaluation of the second order S-matrix for single electron transitions in a potential was first attempted in the 1950s by Brown and co-workers [16]. This calculation scheme requires considerable computing resources, since the multipole expansion of the photon field converges slower and slower for increasing energies; systematic evaluation of the S-matrix element has become practical relatively recently, thanks to wide availability of large scale computing facilities. Extensive calculations based on the S-matrix approach (e.g. [11], [17], [18]) have been performed by Kissel, Pratt and co-workers.

B. Data libraries

Some results of theoretical calculations of photon elastic scattering are publicly available in the form of tabulations distributed as data libraries.

EPDL97 [19] (EPDL Evaluated Photon Data Library, 1997 version), which is part of the ENDF/B-VII.1 [20] evaluated nuclear data file, includes total cross sections, form factors and anomalous scattering factors for atoms with atomic number between 1 and 100, and for photon energies from 1 eV to 100 GeV. The form factors in EPDL97 are the non-relativistic ones calculated by Hubbell [13]; the anomalous scattering factors are by Cullen [21]; the total cross sections derive from calculations combining Thomson scattering, form factors and anomalous scattering factors, which were numerically integrated.

EPDL97 documentation reports rough estimates and qualitative comments about the accuracy of the tabulated data, but it does not document how these estimates were produced. To the best of our knowledge systematic, quantitative validation of EPDL97 coherent scattering data is not documented in the literature.

EPDL97 is extensively used in Monte Carlo simulation; details are given in section III.

The RTAB [22] database encompasses a set of tabulations of photon elastic scattering cross sections, which are the result of various methods of calculation, and of components for their calculations, such as form factors and anomalous scattering factors. The differential cross sections listed in RTAB are based on:

- numerical S-matrix calculations by Kissel and Pratt,
- relativistic form factors,
- non-relativistic form factors by Hubbell et al. [13],
- modified relativistic form factors,
- modified relativistic form factors with angle-independent anomalous scattering factors.

Apart from the data derived from other sources, such as Hubbell's form factors, all the data in the RTAB database have been consistently computed in the same Dirac-Slater potential. The tabulations have been generated on a 97-point grid for scattering angles between 0 and 180 degrees, and on a 56-point grid for energies between 54.3 eV and 2.7541 MeV; they are listed for atomic numbers from 1 to 100.

Two sets of cross sections based on S-matrix tabulations are available in RTAB: one takes into account both the Rayleigh and Thomson scattering amplitudes, which are added coherently, and one is limited to the Rayleigh scattering amplitude. In the following, "S-matrix" or "SM" identify RTAB tabulations involving both amplitudes; whenever tabulations limited to Rayleigh scattering are used, they are explicitly identified in the text.

Comparisons of measured data with S-matrix calculations are reported in some experimental publications, which are limited to the configuration (photon energy, scattering angle and target material) of the experiment they describe. A systematic, quantitative validation of RTAB data is not documented yet in the literature. This database has not been exploited yet in general purpose Monte Carlo systems.

III. PHOTON ELASTIC SCATTERING IN MONTE CARLO CODES

General purpose Monte Carlo codes for particle transport include algorithms for the simulation of Rayleigh scattering,

most of which are based on the form factor approximation; they do not appear to account for other amplitudes involved in photon elastic scattering, apart from the implicit inclusion of Thomson scattering in the calculation of total cross sections by the codes that use EPDL97.

These codes assume that photons interact with free atoms of the medium: this assumption neglects that the molecular structure and the structure of the medium can affect coherent scattering. Some codes provide users the option to directly input tabulated Rayleigh scattering cross sections and form factors, which may account for molecular effects specific to a given material; such tabulations are available for a limited number of materials (e.g. [23]). Photon elastic scattering by molecules is not treated in this paper. The information summarized here concerns models implemented in Monte Carlo codes to describe elastic scattering by non-polarized photons; some Monte Carlo systems also include algorithms for Rayleigh scattering by polarized photons, which are not considered here.

EGS5 [24] and EGS4 [25] calculate total Rayleigh scattering cross sections from the tabulations by Storm and Israel [26], which in turn derive from the integration over angle of equation (2), where form factors by Hanson [27] were used. They sample the coherent scattering angle based on the relativistic form factors by Hubbell and Øverbø [14]. EGSnrc [28] can use three sets of cross section data: those by Storm and Israel as EGS4, and the additional options of EPDL97 and XCOM [29] cross sections.

ETRAN [30] uses the cross sections of the XCOM database, which are based on the relativistic form factors of Hubbell and Øverbø [14], and samples the change in photon direction according to the form factor approximation.

FLUKA [31], [32] simulates Rayleigh scattering based on EPDL97.

ITS [33] calculates total Rayleigh scattering cross sections based on the relativistic form factors by Hubbell and Øverbø [14], but it samples the scattering angle based on the non-relativistic form factors by Hubbell et al. [13].

MCNP5 [34] and MCNPX [35] neglect Rayleigh scattering when the "simple option" of photon transport is chosen; otherwise they also base the simulation on the form factor approximation. They provide different options of Rayleigh scattering data, the most recent of which uses EPDL97; the other options use the older EPDL89 [36] version of EPDL, data from ENDF/B-IV [37] based on non-relativistic form factors by Hubbell et al. [13], and the tabulations by Storm and Israel [26], the latter limited to a few elements with atomic number greater than 83. Nuclear resonance fluorescence, nuclear Thomson scattering and Delbrück scattering are not treated [38].

Penelope [39] 2008 [40] and 2011 [41] versions calculate total Rayleigh scattering cross sections and scattering angles based on EPDL97 [19]; earlier versions exploited analytical approximations [42] to Hubbell's non-relativistic form factors for the calculation of differential and total cross sections. While Penelope 2008 and 2011 documentation [40], [41] states that the total cross sections and form factors used in Penelope are from EPDL97, the tabulations of these quantities

distributed with the Penelope code appear different from those in EPDL97: presumably, the tabulations included in Penelope have been recalculated, or interpolated, over a different energy or momentum transfer grid.

GEANT 3 [43] handled Rayleigh scattering according to empirical formulae derived from EGS3 [44]; they consist of polynomial fits to cross sections by Storm and Israel, and relativistic form factors by Hubbell and Øverbø [14].

The Geant4 toolkit encompasses various implementations of Rayleigh scattering. The latest versions at the time of writing this paper are Geant4 9.4p03 and Geant4 9.5, both released in December 2011 (9.4p03 being the most recent). The Geant4 *G4OpRayleigh* class implements a Rayleigh scattering model only applicable to a particle type identified in Geant4 as “optical photon”, which is an object of the *G4OpticalPhoton* class; this process is not considered in the following analysis, that deals with Geant4 Rayleigh scattering models concerning ordinary photons, which are instances of the *G4Gamma* class.

Functionality for the simulation of Rayleigh scattering of ordinary photons was first introduced [45] in the low energy electromagnetic package [46], [47] of Geant4 0.1 version, based on total cross sections and non-relativistic form factors tabulated in the EPDL97 [19] data library; this modeling approach is identified in Geant4 9.5 as “Livermore Rayleigh model”.

Geant4 also includes two implementations of Rayleigh scattering reengineered from the Penelope [39] Monte Carlo code, respectively equivalent to the Rayleigh scattering algorithms in Penelope 2001 [48] and 2008 [40] versions, the latter also based on EPDL97 as the original Rayleigh scattering implementation available in Geant4. The reengineered Penelope 2008 code uses the tabulations of Rayleigh scattering total cross sections and form factors distributed with Penelope, which, as discussed above, appear different from the native EPDL97 values used by the “Livermore Rayleigh” implementation.

A further Rayleigh scattering simulation model, implemented in the *G4XrayRayleighModel* class, has been first released in Geant4 9.5 version: it is defined in the software release notes as “implementing simplified Rayleigh scattering”, but no further information could be found in Geant4 documentation, nor in the literature, about the physics model underlying this implementation. From the C++ source code, the authors of this paper could evince that this model calculates the total Rayleigh scattering cross section according to an analytical formula involving numerical parameters, and samples the scattering angle according to the distribution of Thomson scattering from a point-like charge.

IV. STRATEGY OF THIS STUDY

An extensive set of simulation models, which are representative of the variety of theoretical approaches documented in the literature, have been evaluated to identify the state-of-the-art of photon elastic scattering in the context of Monte Carlo particle transport. The physics models considered in this analysis involve the implementation of simple formulae in the simulation software or exploit available tabulations of complex theoretical calculations.

The models for photon elastic scattering simulation evaluated in this paper concern total and differential cross sections: in particle transport, the former are relevant to determine the occurrence of the scattering process, while the latter determine the actual outcome of the scattering by defining the angular distribution of the scattered photon at a given energy and for a given target.

All the models subject to study have been implemented in a consistent software design, compatible with the Geant4 toolkit, which minimizes external dependencies to ensure the unbiased appraisal of their intrinsic capabilities.

A wide set of experimental data of photon elastic scattering has been collected from the literature for this study; simulation models are validated through comparison with these measurements. The compatibility with experiment for each model, and the differences in compatibility with experiment across the various models, are quantified by means of statistical methods.

The measurements of photon elastic scattering reported in the literature mainly concern differential cross sections; therefore the validation process is focused on this observable. Due to the scarcity of total cross section measurements in the literature, the capability of the simulation models to calculate total cross sections consistent with experiment can be directly tested only over a small data sample; nevertheless, it can be indirectly inferred for total cross sections deriving from the integration of validated differential cross sections.

The validation of the physics capabilities of the simulation models is complemented by the evaluation of their computational performance.

A. Simulation models

The simulation models of differential cross section analyzed in this study implement calculations based on second order S-matrix and on the form factor approximation; they are summarized in Table I. Some of these simulation models represent novel approaches with respect to those so far available in Geant4 and in other general purpose Monte Carlo codes; among them, the paper examines whether a model based on S-matrix calculations, which constitutes a more consistent theoretical approach, but requires more complex computational operations, would be sustainable in the context of Monte Carlo particle transport.

Various simulation models are based on the non-relativistic form factors by Hubbell et al. [13]: they are identified in Table I as “EPDL”, “NF”, “Penelope 2001” and “Penelope 2008”. They use different tabulations of the form factors as a function of momentum transfer, or different algorithms to sample the scattered photon direction based on the form factors. The model identified as “EPDL” uses non relativistic form factors as they are tabulated in EPDL97; it corresponds to the original Rayleigh scattering simulation method in Geant4 low energy electromagnetic package [45], which has been reengineered in the context of the policy-based class design described in section IV-B. The models identified in this paper as “Penelope 2001” and “Penelope 2008” correspond to algorithms reengineered from the respective Penelope versions: as mentioned in section III, the Penelope 2008 model is

TABLE I
SIMULATION MODELS OF PHOTON ELASTIC SCATTERING: DIFFERENTIAL CROSS SECTIONS

Identifier	Underlying theoretical approach	Tabulated data source
EPDL	Non-relativistic form factors	EPDL97
EPDLASF	Non-relativistic form factors + anomalous scattering factors	EPDL97
Penelope 2001	Parameterization of non-relativistic form factors (as in Penelope 2001)	-
Penelope 2008	Non-relativistic form factors (as in Penelope 2008-2011)	Retabulated EPDL97
RF	Relativistic form factors	RTAB
NF	Non-relativistic form factors	Hubbell 1975, as reported in RTAB
MF	Modified form factors	RTAB
RFASF	Relativistic form factors and anomalous scattering factors	RTAB
MFASF	Modified form factors and anomalous scattering factors	RTAB
SM	Second order S-matrix	RTAB

based on the EPDL97 data library, although re-tabulated over a different grid, while the Penelope 2001 model exploits analytical approximations to Hubbell’s non-relativistic form factors. The model identified in this paper as “NF” exploits the non-relativistic form factors listed in RTAB.

Models based on relativistic and modified form factors, based on RTAB tabulations, are respectively identified as “RF” and “MF”. To the best of the authors’ knowledge, modified form factors have not been used yet in general purpose Monte Carlo codes.

Additionally, calculations accounting for anomalous scattering factors along with form factors are evaluated: the “RFASF” and “MFASF” models are based on RTAB tabulations, while the “EPDLASF” model exploits the anomalous scattering factors included in EPDL97, which have not been used yet in any of the general-purpose Monte Carlo systems relying on EPDL97.

The model identified as “SM” is based on RTAB tabulations of second order S-matrix calculations. This model accounts for the sum of two coherent amplitudes: the so-called Rayleigh amplitude and nuclear Thomson scattering. A model based on S-matrix calculations limited to the Rayleigh scattering amplitude is discussed in section V-D. To the best of the authors’ knowledge, this paper documents the first implementation based on S-matrix calculations for the simulation of photon elastic scattering by a general-purpose Monte Carlo system.

Total cross sections are calculated corresponding to all the models listed in Table I; those that are highlighted as most relevant by the validation analysis of differential cross sections in section V-B are discussed in detail in section V-C. Furthermore, the total cross sections calculated by interpolation of Storm and Israel [26] tables, by the XCOM Photon Cross Section Database distributed by NIST (National Institute of Standards), by Brennan and Cowan [49] parameterizations of McMaster’s [50] cross sections (commonly used in photon science), and by Geant4 *G4XrayRayleighModel* are evaluated. The energy ranges covered by these compilations are respectively 1-100 MeV (Storm and Israel), 0.03-695 keV (Brennan and Cowan) and 1 keV to 100 GeV (XCOM). The total cross section models examined in this paper are summarized in Table II.

Tabulations of total Rayleigh scattering cross sections are directly available in EPDL97, XCOM and [26]; tabulations for other physics models have been produced on the same energy

grid as EPDL97 to facilitate the comparison of the various models. The tabulations associated with the simulation models based on RTAB listed in Table I were produced by integrating the corresponding differential cross sections over the angle.

B. Software environment

All the physics models evaluated in this paper have been implemented in the same software environment, which is compatible with Geant4; computational features specific to the original physics algorithms have been preserved as much as possible. The uniform software configuration ensures an unbiased appraisal of the intrinsic characteristics of the various physics models. The correctness of implementation has been verified prior to the validation process to ensure that the software reproduces the physical features of each model consistently.

The software adopts a policy-based class design [51]; this technique was first introduced in a general-purpose Monte Carlo system in [52]. This programming paradigm supports the provision of a series of alternative physics models for Monte Carlo transport, characterized by high granularity, which can be used interchangeably with great versatility, without imposing the burden of inheritance from a pre-defined interface, since policies are syntax-oriented, rather than signature-oriented.

Two policies have been defined for the simulation of photon elastic scattering, corresponding to the calculation of total cross section and to the generation of the scattered photon; they conform to the prototype design described in [54], [55]. A photon elastic scattering process, derived from the *G4VDiscreteProcess* class of Geant4 kernel, acts as a host class for these policy classes. All the simulation models implemented according to this policy-based class design are compatible for use with Geant4, since Geant4 tracking handles all discrete processes polymorphically through the *G4VDiscreteProcess* base class interface.

A single policy class calculates total cross sections for all the physics models that exploit tabulations; alternative tabulations, corresponding to different physics models, are managed through the file system. Specific policy classes implement the analytical calculations of total cross sections as in Penelope 2001 and *G4XrayRayleighModel*.

Two alternative policy classes sample the direction of the scattered photon utilizing the form factor approximation: they

TABLE II
SIMULATION MODELS OF PHOTON ELASTIC SCATTERING: TOTAL CROSS SECTIONS

Identifier	Method	Source
EPDL	Non-relativistic form factors with anomalous scattering factors	EPDL97
Penelope 2001	Analytical model	Penelope 2001
MFASF	Integration of differential cross sections based on modified form factors with anomalous scattering factors	RTAB
SM	Integration of cross sections based on second order S-matrix	RTAB
XCOM	Based on form factor approximation	NIST
Storm	Storm and Israel tabulations	[26]
Brennan	Brennan and Cowan's parameterization of McMaster et al. cross sections	[49]
G4std	Parameterization in the Geant4 <i>G4XrayRayleighModel</i> class	Not documented

differ by the sampling algorithm, respectively based on the inverse transform method and on acceptance-rejection sampling [53]. Both can be used with any tabulated form factors, which are managed through the file system.

A dedicated policy class deals with the generation of the scattered photon based on S-matrix calculations; the scattering angle is sampled based on the inverse transform sampling method.

Dedicated policy classes generate the scattered photon according to the analytical formulations used in Penelope 2001 and *G4XrayRayleighModel*.

The final state generation based on the form factor approximation involves one-dimensional interpolations only, while the use of S-matrix calculations requires bi-dimensional interpolation of RTAB data. Interpolation algorithms are discussed in section V-F.

The software design adopted in this study ensures greater flexibility than the design currently adopted in Geant4 electromagnetic package, since it allows independent modeling (and test) of total cross section calculation and photon scattering generation. Since policy classes are characterized by a single responsibility and have minimal dependencies on other parts of the software, the programming paradigm adopted in this study also facilitates the validation of physics models: validation tests involve only the instantiation of an object of the policy class and the invocation of the member function implementing the policy, therefore they expose only the intrinsic features of the physics models, excluding possible effects on physics behaviour due to other parts of the Monte Carlo system. Equivalent validation tests of physics models as currently implemented in Geant4 require instead a full scale simulation application, including the creation of a geometry model even when it is conceptually redundant (e.g. to validate a cross section calculation).

C. Experimental data

Experimental data for the validation of the simulation models were collected from a survey of the literature.

The sample of experimental differential cross sections consists of approximately 4500 measurements [3], [58]- [158], which concern 69 target atoms and span energies from 5.41 keV to 39 MeV, and scattering angles from 0.5 to 165 degrees. An overview of this data sample is summarized in Tables III and IV.

Experimental total cross section data are scarce in the literature. To the best of our efforts we could retrieve only a journal

publication [159] reporting a measurement at 661.6 keV for four elements: barium, tungsten, lead and bismuth. A larger set of measurements by the same group as [159], concerning 18 target elements and two photon energies (279.2 keV and 661.6 keV), is documented in [160]; this reference includes the four values published in [159]. The experimental errors reported in [160] vary between 3% and 6% for the measurements at 661.6 keV, and between 0.3% and 0.5% for the data at 279.2 keV: since the reported precision of the two sets of measurements in similar experimental conditions differs by an order of magnitude, and better than 1% precision appears inconsistent with typical experimental errors in the field documented in the literature, one may wonder whether some of the experimental uncertainties listed in [160] could be affected by a typographical slip.

It is worthwhile to note that the available experimental differential cross section data are too scarce to calculate total cross sections based on them. Therefore they could not be exploited for the validation of theoretical total cross section models.

A small sample of experimental measurements of photon elastic scattering at the electronvolt scale has been retrieved; data at such low energy are scarce in the literature, and consist mostly of measurements of molecular cross sections, which are outside the scope of this paper. A few measurements of absolute total cross sections, that concern atomic gaseous targets (mostly noble gases) in the energy range of approximately 1-10 eV, have been retrieved in the literature: the intrinsic physical characteristics of these data are congruous for comparison with calculations performed in independent particle approximation, since molecular effects, which become important at low energies, are expected to be minimized in atomic gaseous targets. Some of these data involved normalizations to other values to obtain absolute cross sections: these manipulations can be source of systematic effects and, if the normalization is based on theoretical references, would make the data inappropriate for the validation of simulation models. Although this very low energy data sample is too limited to serve for proper simulation validation, it enables at least a qualitative appraisal of EPDL97 cross sections, that extend down to 1 eV.

Some experimental cross sections have been published only in graphical form; numerical values were digitized from the plots by means of the Engauge [56] software. The error introduced by the digitization process was estimated by digitizing a few plots, whose numerical content is explicitly reported in the related publications. The reliability of the

TABLE III
SUMMARY OF THE EXPERIMENTAL DATA USED IN THE VALIDATION ANALYSIS: ATOMIC NUMBERS 3-72

Z	Element Symbol	Energy range (keV)	Angle range (degrees)	Sample size	References
3	Li	1600	124	1	[58]
4	Be	59.54	45	9	[103]
5	B	145.4	2.03	4	[91], [147]
6	C	22.1–145.4	2.03–133	13	[91], [97], [111], [141], [147]
7	N	145.4	2.03	1	[147]
12	Mg	22.16–59.54	90–121	4	[133], [148], [149]
13	Al	14.93–1600	1.6–145	86	[58], [66], [69], [70], [76], [83], [91], [96], [98], [103], [107], [127], [132]–[135], [139]–[142], [148], [149], [153], [156]
14	Si	17.44–59.54	90–121	3	[97], [131], [149]
16	S	22.1–59.54	121–133	2	[111], [149]
21	Sc	17.44–30.85	90–90	2	[131], [135]
22	Ti	17.44–59.54	10–160	18	[75], [113], [115], [127], [131], [135], [148], [149]
23	V	17.44–59.54	10–160	17	[76], [97], [113], [115], [131], [135], [149]
24	Cr	17.44–33.29	90–90	9	[131], [133]–[135]
25	Mn	17.44–33.29	90–90	4	[131], [133], [135]
26	Fe	6.4–1120.5	2.72–130	38	[75], [81], [88], [97], [115], [127], [131], [134], [135], [141], [148], [149]
27	Co	17.44–59.54	10–160	13	[113], [127], [131], [135], [148]
28	Ni	7.47–81	45–145	22	[66], [69], [75], [115], [127], [131], [133], [135], [148], [149]
29	Cu	8.04–1408.1	1.02–165	306	[64], [65], [73], [75], [78], [81], [83]–[87], [91], [94], [96]–[98], [105], [109], [114], [115], [122]–[124], [127], [129], [131]–[135], [139]–[142], [147]–[150], [153], [156]
30	Zn	8.63–661.6	10–165	87	[75], [77], [83], [85]–[88], [93], [97], [112], [113], [115], [127], [131], [135], [145], [148], [149], [152]
31	Ga	16.58	90	1	[133]
32	Ge	9.8–59.54	90–133	4	[75], [111], [149]
33	As	22.1	133	1	[111]
34	Se	22.1	133	1	[111]
36	Kr	59.54	20	11	[151]
37	Rb	22.1	133	1	[111]
38	Sr	14.14–30.85	90–90	10	[75], [132], [134], [135]
39	Y	17.44–59.54	10–160	19	[113], [131], [133], [135], [139], [140], [148], [149]
40	Zr	13.95–661.6	10–165	67	[75], [80], [85]–[87], [113], [115], [120], [125]–[127], [134], [135], [148], [149]
41	Nb	13.95–59.54	10–165	66	[75], [80], [85]–[88], [113], [115], [127], [131], [135], [148], [149]
42	Mo	13.95–1408.1	2–165	220	[64], [65], [67], [75], [76], [80], [85]–[87], [97], [98], [112]–[115], [121], [123], [124], [127], [133], [135], [140], [145], [148]–[150], [152], [155], [156]
44	Ru	22.16–59.54	90–121	2	[75], [149]
45	Rh	22.16–59.54	117–121	2	[148], [149]
46	Pd	5.41–59.54	90–130	18	[115], [127], [131], [133]–[135], [137], [148], [149]
47	Ag	5.41–661.6	5.12–165	125	[59], [60], [63]–[65], [75], [85]–[87], [94], [111], [113], [123], [124], [131], [133]–[135], [137], [149], [150]
48	Cd	5.41–1600	2.4–165	173	[58], [63]–[65], [75], [76], [83]–[87], [91], [94], [113], [115], [121], [123], [124], [127], [129], [131]–[133], [135]–[137], [148]–[150]
49	In	5.41–1302	1.02–165	63	[75], [85]–[87], [105], [115], [127], [131], [133], [135]–[137], [139], [148], [149]
50	Sn	5.41–1408.1	1.03–165	405	[59]–[61], [64], [65], [71]–[76], [81], [85]–[87], [92], [93], [96], [98], [99], [109], [112]–[116], [119]–[127], [131], [133], [135]–[137], [141], [145], [147]–[150], [152], [153], [155]
51	Sb	5.41–59.54	90–131	24	[75], [131], [133], [136], [137], [149]
52	Te	22.1–59.54	121–133	2	[111], [149]
53	I	661.6–1120.5	95–110	4	[59], [81]
54	Xe	59.54–661.6	3.02–120	25	[95], [151]
55	Cs	17.44	90	1	[131]
56	Ba	17.44–1120.5	57.5–133	15	[63], [75], [81], [111], [112], [131], [135], [149]
57	La	17.44–661.6	1.77–90	3	[131], [135], [147]
58	Ce	14.93–59.54	90–131	6	[75], [131], [132], [135]
59	Pr	14.93–279.2	90–90	10	[123], [124], [131]–[133], [135], [150]
60	Nd	22.16–661.6	1.77–135	11	[75], [147], [152]
62	Sm	14.93–279.2	90–133	13	[75], [111], [115], [123], [124], [132], [133], [135], [150]
63	Eu	17.44	90	1	[131]
64	Gd	17.44–320	10–160	34	[62], [75], [112], [113], [115], [123], [124], [130], [131], [135], [148]–[150]
65	Er	59.54–320	45–121	11	[130], [149]
66	Dy	16.58–661.6	1.77–160	36	[62], [75], [113], [115], [123], [124], [127], [130], [131], [133], [135], [147]–[150]
67	Ho	16.58–279.2	10–160	20	[75], [111]–[113], [123], [124], [131], [133], [135], [149], [150]
68	Er	16.58–59.54	10–165	22	[62], [113], [115], [121], [131], [133], [135], [148], [149]
69	Tm	22.1	133	1	[111]
70	Yb	16.58–320	10–160	35	[62], [75], [111]–[113], [115], [123], [124], [130], [131], [133], [135], [149], [150], [156]
72	Hf	22.16–511	0.5–160	13	[62], [75], [102], [113]

TABLE IV
SUMMARY OF THE EXPERIMENTAL DATA USED IN THE VALIDATION ANALYSIS: ATOMIC NUMBERS 73-92

Element <i>Z</i>	Symbol	Energy range (keV)	Angle range (degrees)	Sample size	References
73	Ta	13.95-1408.1	0.5-165	295	[62], [66], [67], [69], [75], [77], [85]–[87], [98], [102], [105], [112]–[114], [119], [120], [123]–[127], [129], [145], [148]–[150], [152], [155], [156]
74	W	13.95-1408.1	0.5-165	151	[59], [60], [63]–[65], [78], [85]–[87], [102], [112], [113], [123], [124], [127], [148]–[150], [154]
75	Re	22.16-511	0.5-121	3	[102], [148], [149]
77	Ir	22.16-511	0.5-160	11	[102], [113], [148], [149]
78	Pt	5.41-1120.5	0.5-160	100	[63], [94], [102], [112], [113], [119], [120], [127], [131]–[133], [135], [137], [138], [148], [149]
79	Au	5.41-511	0.5-160	108	[66], [69], [70], [75], [89], [97], [102], [107], [112], [113], [115], [131]–[135], [137]–[140], [145], [146], [148], [149], [156]
80	Hg	22.1-1600	0.5-135	16	[58], [59], [68], [81], [102], [111], [112], [144], [147], [149]
81	Tl	22.1-511	0.5-133	3	[102], [111], [112]
82	Pb	5.41-1613	0.5-160	797	[3], [59]–[61], [64]–[79], [81]–[84], [89], [91]–[94], [96]–[102], [104], [107]–[110], [112]–[117], [119], [120], [122]–[129], [131]–[135], [137]–[140], [142]–[150], [152], [153], [155], [156], [158]
83	Bi	22.16-511	0.5-131	9	[70], [75], [102], [107], [112], [148], [149]
90	Th	22.16-661.6	0.5-125	11	[102], [112], [123], [124], [147]–[150]
92	U	22.16-1613	0.5-160	262	[63], [75], [92], [93], [100]–[102], [106], [110], [112]–[114], [118], [123], [124], [148]–[150], [155]

digitized cross section values is hindered by the difficulty of appraising the experimental points and their error bars in plots that may span several orders of magnitude in logarithmic scale; these digitized data were not used in the validation analysis, if found incompatible with other measurements in the same experimental configuration (target element, incident photon energy and measured angle) reported in the literature in numerical form.

Large discrepancies are evident in some of the experimental data; systematic effects are likely present in some cases, where the Wald-Wolfowitz test [57] detects sequences of positive or negative differences between data samples originating from different experimental groups, which are incompatible with randomness. Experimental data exhibiting large discrepancies with respect to other measurements in similar configurations, that hint to the presence of systematic effects, are excluded from the validation process.

Correct estimate of experimental errors is a concern in the validation process, since unrealistic estimation of the experimental errors may lead to incorrect conclusions regarding the rejection of the null hypothesis in tests whose statistic takes into account experimental uncertainties explicitly. Although technological developments have contributed to improved precision of measurement, it has been remarked that in some circumstances estimates of experimental uncertainties of the order of 5% or less reported in the literature may be optimistic [5]. Experimental measurements claiming much smaller uncertainties than similar ones have been critically evaluated in the analysis process; effects related to the validation of simulation models are discussed in section V-B.

D. Data analysis method

The evaluation of the simulation models performed in this study has two objectives: to validate them quantitatively, and to compare their relative capabilities.

The scope of the software validation process is defined according to the guidelines of the pertinent IEEE Standard

[161], which conforms to the life cycle process standard defined in ISO/IEC Standard 12207 [162]. For the problem domain considered in this paper, the validation process provides evidence that the software models photon-atom elastic scattering consistent with experiment.

A quantitative analysis, based on statistical methods, is practically possible only for the validation of differential cross sections, for which a large sample of experimental data is available. The analysis of differential cross sections is articulated over two stages: the first one estimates the compatibility between the values calculated by each simulation model and experimental data, while the second exploits the results of the first stage to determine whether the various models exhibit any significant differences in their compatibility with experiment.

The first stage encompasses a number of test cases, each one corresponding to a photon energy for which experimental data are available. For each test case, cross sections calculated by the software are compared with measured ones by means of goodness-of-fit tests; the null hypothesis in the tests is defined as the equivalence of the simulated and experimental data distributions subject to comparison. The Statistical Toolkit [163], [164] is exploited for these tests. The level of significance of the tests described in the following sections is 0.01, unless differently stated; it means that the null hypothesis is rejected whenever the p-value resulting from the test statistic is smaller than 0.01.

The goodness-of-fit analysis is primarily based on the χ^2 test [165]. Among goodness-of-fit tests, this test has the peculiarity of taking into account experimental uncertainties explicitly; therefore the test statistic is sensitive to their correct appraisal. Three tests based on the empirical distribution function, the Kolmogorov-Smirnov [166], [167], Anderson-Darling [168], [169] and Cramer-von Mises [170], [171] tests, have also been applied; nevertheless, as documented in the following sections, they exhibit limited discriminant power over the data sample of this study. In this context one may want to recall that the power of goodness-of-fit tests is still object of active research in statistics.

The “efficiency” of a physics model is defined as the fraction of test cases in which the χ^2 test does not reject the null hypothesis at 0.01 level of significance: it quantifies the capability of that simulation model to produce results statistically consistent with experiment over the whole set of test cases, which in physical terms means over the whole energy range of the experimental data sample involved in the validation process.

The second stage of the statistical analysis quantifies the differences of the simulation models in compatibility with experiment. It consists of a categorical analysis based on contingency tables, which derive from the results of the χ^2 test: the outcome of this test is classified as “fail” or “pass”, according respectively to whether the hypothesis of compatibility of experimental and calculated data is rejected or not. The categorical analysis takes as a reference the simulation model exhibiting the largest efficiency at reproducing experimental data; the other models are compared to it, to determine whether they exhibit statistically significant differences of compatibility with measurements.

The null hypothesis in the analysis of a contingency table assumes the equivalent compatibility with experiment of the models it compares. Contingency tables are analyzed with Fisher’s exact test [172] and with the χ^2 test applying Yates’ continuity correction [173]; the latter ensures meaningful results when one or more cells of the table have few entries. Pearson’s χ^2 test [174] is also performed on contingency tables, when their content is consistent with its applicability. The use of different tests in the analysis of contingency tables contributes to the robustness of the results, as it mitigates the risk of introducing systematic effects, which could be due to the peculiar mathematical features of a single test.

The significance level for the rejection of the null hypothesis in the analysis of contingency tables is 0.05, unless differently specified.

The scarcity of experimental measurements of elastic scattering total cross sections in the literature hinders the validation of simulation models through similar statistical analysis methods: only qualitative general considerations can be made, while quantitative assessments are limited by the small sample of published experimental data. Nevertheless, the results of the analysis of differential cross sections contribute indirectly to assess the validity of total cross sections, since some of the implemented total cross section models derive from the integration of the differential cross sections subject to validation.

V. RESULTS

The following sections report the results of the comparison of differential and total cross sections with experimental data, and of the evaluation of the computational performance of the various simulation models.

A. General features

Elastic scattering cross sections vary by several orders of magnitude over the data sample involved in the validation analysis. Cross sections decrease as a function of photon energy

and scattering angle, and are larger for heavy elements: these trends are illustrated in Figs. 1 and 2, that show experimental photon elastic scattering measurements along with the values calculated by representative simulation models for the same energy and scattering angle settings.

Experimental differential cross sections are the result of all the physics processes that contribute to photon elastic scattering, while the simulation models evaluated in this paper account for the Rayleigh scattering amplitude only or, in the case of the model based on S-matrix calculations, for the sum of Rayleigh and Thomson scattering amplitudes. This feature is evident in Fig. 3, which includes some of the higher energy measurements in the experimental data sample: other processes, such as Delbrück scattering, should be taken into account in the simulation, along with Rayleigh scattering, to model photon elastic scattering accurately at higher energies. The plots also expose some characteristics of the experimental data: systematic effects affecting some of the measurements, and the presence of outliers in the experimental sample.

The distributions in Figs. 4 and 5 illustrate the difference between calculated and measured differential cross sections, for a few representative models: two options based on the form factor approximation, respectively using the form factors tabulated in EPDL97 and modified form factors with anomalous scattering factors, and the model based on S-matrix calculations. Fig. 4 shows the relative difference between simulated and experimental values. Fig. 5 accounts for the different precision of the data in the experimental sample: it represents the difference between calculated and experimental differential cross sections in units of standard deviations, i.e. of the uncertainties associated with the experimental measurements. These plots are limited to photon energies up to 1.5 MeV, since, as shown in Fig. 3, at higher energies other processes should be taken into account to describe photon elastic scattering. The long tails of the distributions in Figs. 4 and 5 are the result of multiple factors: neglect of amplitudes other than Rayleigh scattering in some of the calculations, inadequacy of the simulation models, and contamination of the experimental sample by measurements affected by systematic effects and outliers. One can observe in Fig. 4 that the distribution of the relative differences between the differential cross sections calculated by the models and experimental data is narrower for the S-matrix model, while it is wider for the cross sections based on EPDL and on modified form factors with anomalous scattering factor corrections.

The one sample t-test [175] for the hypothesis of null mean difference between simulation and experiment confirms the qualitative features observed in Figs. 4 and 5. Fig. 6 shows the 99% confidence intervals for the true mean difference associated with the various models: the model based on S-matrix calculations is the only one for which the confidence interval includes zero. The hypothesis of null mean difference from experiment equal to zero is rejected for all the cross section models with 0.001 significance, with the exception of the model based on S-matrix calculations, for which the p-value resulting from the t-test is 0.500.

The algorithm for Rayleigh scattering simulation reengineered from Penelope 2008-2011 versions produces very

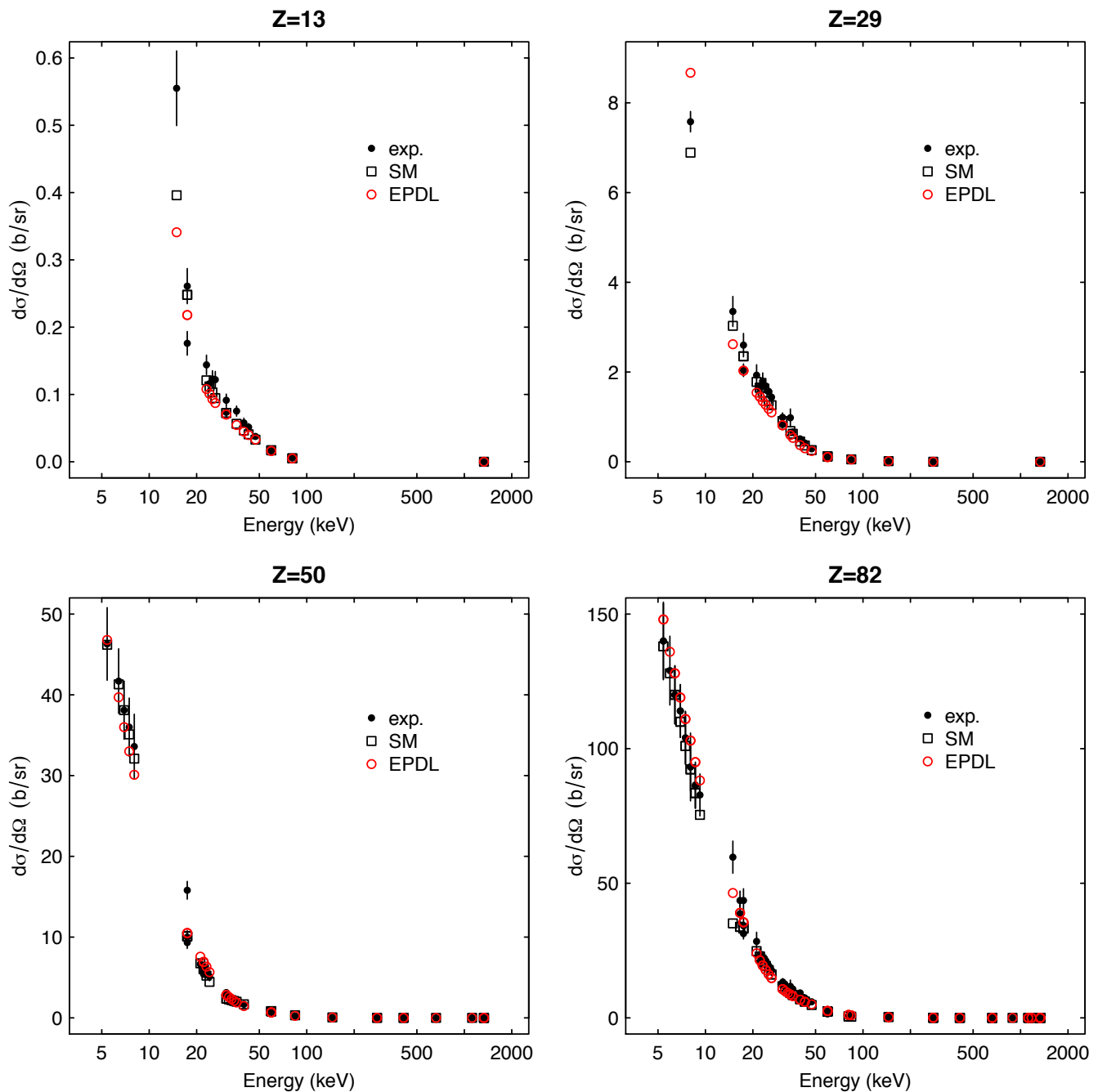


Fig. 1. Differential cross section as a function of energy at $\theta = 90^\circ$ for aluminium, copper, tin and lead: experimental measurements (black circles), calculations based on S-matrix (SM, black empty squares) and on EPDL (red circles). The sources of experimental data are documented in Tables III and IV.

similar results to the algorithm originally developed in [45], which corresponds to the policy class identified in this paper as EPDL: in fact, both of them are based on EPDL97 data. Figs. 7 and 8 show the relative difference between the total and differential cross sections calculated by these two models; the small differences are due to the different reference grids used by the two models in the respective tabulations of total cross sections and non-relativistic form factors, which affect the values calculated by interpolation. The difference of resulting total cross sections appears insignificant, considering that the scale of Fig. 7 extends to relative differences up to 0.05%,

while the distribution of differences between differential cross sections, shown in Fig. 8, is wider, having a standard deviation of 1%: the effect of these differences on the accuracy of the two models is quantitatively estimated in section V-B.

B. Differential cross sections

The analysis of differential cross sections is articulated over the set of discrete energies for which experimental data are available. The p-values resulting from the χ^2 test applied to the data samples corresponding to each energy are listed

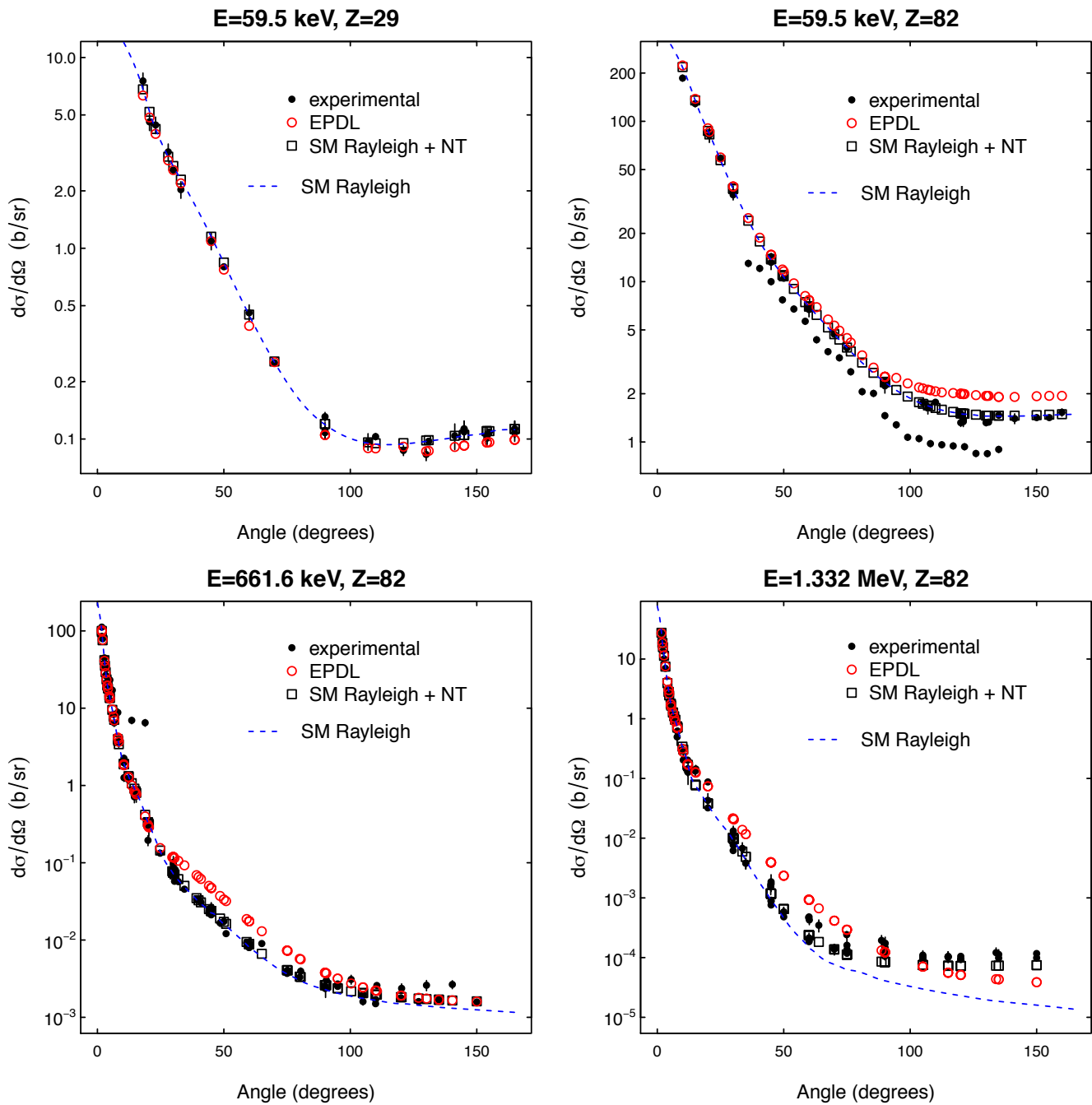


Fig. 2. Differential cross section as a function of scattering angle for representative energies and target elements: experimental measurements (black circles), calculations based on S-matrix (SM, black empty squares) and on EPDL (red circles). The S-matrix calculations account for Rayleigh scattering and nuclear Thomson scattering; S-matrix calculations limited to the Rayleigh scattering amplitude are shown as a blue dashed line. The sources of experimental data are documented in Tables III and IV.

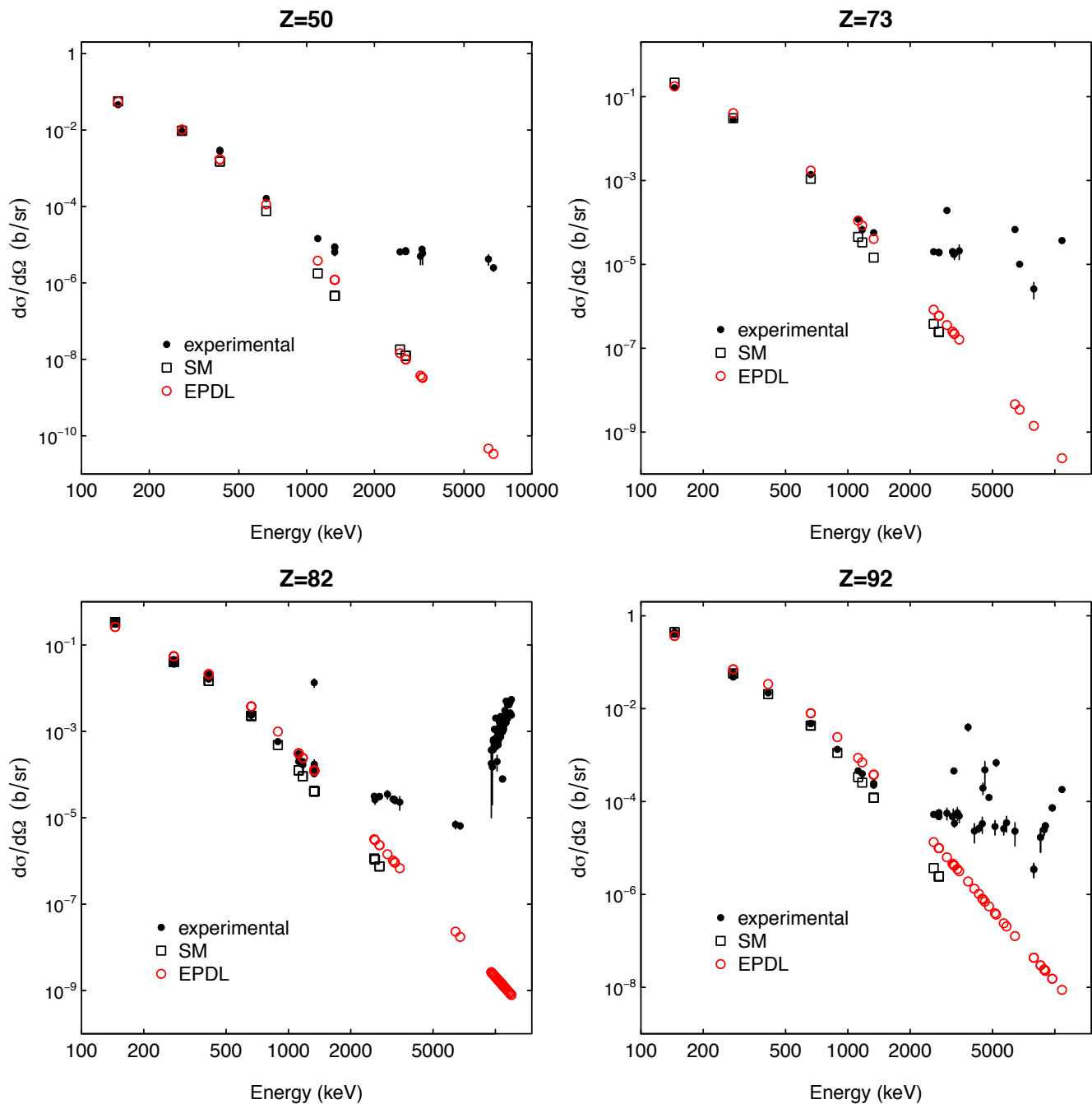


Fig. 3. Differential cross section as a function of energy at $\theta = 90^\circ$ for tin, tantalum, lead and uranium: experimental measurements (black circles), calculations based on S-matrix (SM, black empty squares) and on EPDL (red circles). The sources of experimental data are documented in Tables III and IV.

in Tables V, VI and VII, respectively concerning the whole angular range, data up to 90° and above 90° (backscattering).

The efficiency of the various simulation models is reported in Table VIII. The results are listed for three data samples: the whole experimental data collection, the data for scattering angles up to 90° and above 90° . The simulation model based on the interpolation of RTAB S-matrix calculations, indicated in the tables as SM, stands out as the one exhibiting the largest efficiency in all test configurations.

Three test cases for which the χ^2 test rejects the hypothesis of compatibility between the S-matrix model and experimental

data involve measurements from a single reference; due to the lack of other experimental data in the same configuration, one cannot exclude that the incompatibility between S-matrix calculations and experiment could be ascribed to systematic effects in the data, rather than to deficiencies of the simulation model. The exclusion of these three test cases from the analysis slightly increases the efficiencies of all the simulation models (e.g. 0.81 ± 0.05 for the S-matrix model and 0.40 ± 0.05 for the EPDL-based model, over the whole angular range), nevertheless it does not substantially change the conclusions one can draw from the χ^2 test.

TABLE VII
DIFFERENTIAL CROSS SECTIONS: P-VALUES RESULTING FROM THE χ^2 TEST, DATA SAMPLE ABOVE 90°

E (keV)	Penelope 2001	Penelope 2008-2011	EPDL	EPDL ASF	SM	RF	NF	MF	MF ASF	RF ASF
13.95	< 0.001	< 0.001	< 0.001	0.002	0.154	< 0.001	< 0.001	< 0.001	0.046	0.064
17.75	< 0.001	< 0.001	< 0.001	< 0.001	0.105	< 0.001	< 0.001	< 0.001	0.009	0.025
22.1	< 0.001	< 0.001	< 0.001	< 0.001	0.010	< 0.001	< 0.001	< 0.001	< 0.001	< 0.001
26.36	< 0.001	< 0.001	< 0.001	< 0.001	< 0.001	< 0.001	< 0.001	< 0.001	0.772	0.758
59.54	< 0.001	< 0.001	< 0.001	< 0.001	< 0.001	< 0.001	< 0.001	< 0.001	< 0.001	0.001
81	< 0.001	< 0.001	< 0.001	< 0.001	0.365	< 0.001	< 0.001	< 0.001	0.004	0.082
88	< 0.001	< 0.001	< 0.001	< 0.001	< 0.001	< 0.001	< 0.001	< 0.001	< 0.001	< 0.001
145.4	< 0.001	< 0.001	< 0.001	< 0.001	< 0.001	< 0.001	< 0.001	< 0.001	< 0.001	< 0.001
279.2	< 0.001	< 0.001	< 0.001	< 0.001	0.096	< 0.001	< 0.001	< 0.001	< 0.001	< 0.001
317	< 0.001	< 0.001	< 0.001	0.019	< 0.001	0.200	< 0.001	< 0.001	< 0.001	< 0.001
411.8	< 0.001	< 0.001	< 0.001	< 0.001	0.034	< 0.001	< 0.001	< 0.001	< 0.001	< 0.001
468.1	0.015	0.047	0.037	< 0.001	0.368	< 0.001	0.045	< 0.001	< 0.001	< 0.001
661.6	< 0.001	< 0.001	< 0.001	< 0.001	0.508	< 0.001	< 0.001	< 0.001	< 0.001	< 0.001
889	< 0.001	< 0.001	< 0.001	< 0.001	0.940	< 0.001	< 0.001	< 0.001	< 0.001	< 0.001
1120	< 0.001	< 0.001	< 0.001	< 0.001	< 0.001	< 0.001	< 0.001	< 0.001	< 0.001	< 0.001
1173	< 0.001	< 0.001	< 0.001	< 0.001	0.022	< 0.001	< 0.001	< 0.001	< 0.001	< 0.001
1332	< 0.001	< 0.001	< 0.001	< 0.001	< 0.001	< 0.001	< 0.001	< 0.001	< 0.001	< 0.001

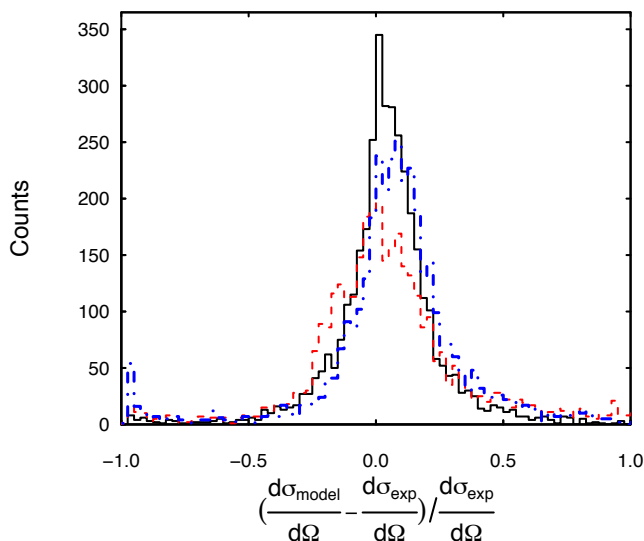


Fig. 4. Relative difference between the differential cross sections calculated by simulation models and the corresponding experimental measurements: calculations based on based S-matrix (SM, solid black line), EPDL (dashed red line) and MFASF form factors (dot-dashed blue line). The plot is limited to photon energies up to 1.5 MeV

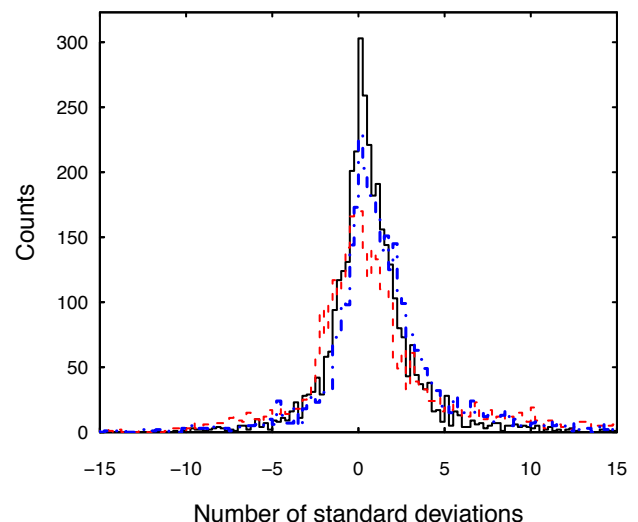


Fig. 5. Difference between the differential cross sections calculated by simulation models and the corresponding experimental measurements, expressed in terms of number of standard deviations (experimental uncertainties): calculations based on based S-matrix (SM, solid black line), EPDL (dashed red line) and MFASF form factors (dot-dashed blue line). The plot is limited to photon energies up to 1.5 MeV

Several cases of inconsistency between simulation models and experimental data concern measurements at photon energies close to the K or L shell electron binding energies of target atom; a number of them involve measurements for which relatively small experimental uncertainties are reported, that could have been underestimated. The same analysis has also been performed on a sample that excludes these data; its results, which are reported in Table IX, confirm the same general trend observed in Table VIII. The larger relative increase in efficiency of the models based on RTAB observed in this analysis with respect to the effect on other models suggests that this database might have adopted a coarse grid for its tabulations, that degrades the accuracy of interpolation in sensitive areas.

The compatibility between simulation models and experimental data has been evaluated also through the Kolmogorov-Smirnov, Anderson-Darling and Cramer-von Mises goodness-of-fit tests. The results, listed in Table X, suggest that these tests exhibit scarce sensitivity to differences between the simulation models and the experimental data subject to comparison.

The relative accuracy of the various simulation models is compared by contingency tables based on the outcome of the χ^2 test. In these comparisons the model based on the S-matrix, which exhibits the largest efficiency, is taken as a reference; contingency tables examine whether the results of the χ^2 test over other models are statistically equivalent to those of this model.

Since several general purpose Monte Carlo systems base

TABLE VIII
 χ^2 TEST OUTCOME: TEST CASES COMPATIBLE WITH EXPERIMENT AT 0.01 SIGNIFICANCE LEVEL

Test		Penelope 2001	Penelope 2008-2011	EPDL	EPDL ASF	SM	RF	NF	MF	MF ASF	RF ASF
all	Test cases	71	71	71	71	71	71	71	71	71	71
	Pass	19	27	27	18	55	18	25	35	37	34
	Fail	52	44	44	53	16	53	46	36	34	37
	Efficiency	0.27	0.38	0.38	0.25	0.77	0.25	0.35	0.49	0.52	0.48
	Error	± 0.05	± 0.06	± 0.06	± 0.05	± 0.06	± 0.05	± 0.06	± 0.06	± 0.06	± 0.06
$\theta \leq 90^\circ$	Test cases	67	67	67	67	67	67	67	67	67	67
	Pass	19	27	27	18	55	18	25	35	36	32
	Fail	48	40	40	49	12	49	42	32	31	35
	Efficiency	0.28	0.40	0.40	0.27	0.82	0.27	0.37	0.52	0.54	0.48
	Error	± 0.05	± 0.06	± 0.06	± 0.05	± 0.05	± 0.05	± 0.06	± 0.06	± 0.06	± 0.06
$\theta > 90^\circ$	Test cases	17	17	17	17	17	17	17	17	17	17
	Pass	1	1	1	1	10	1	1	0	2	4
	Fail	16	16	16	16	7	16	16	17	15	13
	Efficiency	0.06	0.06	0.06	0.06	0.59	0.06	0.06	< 0.06	0.12	0.24
	Error	± 0.06	± 0.06	± 0.06	± 0.06	± 0.12	± 0.06	± 0.06		± 0.08	± 0.10

TABLE IX
 χ^2 TEST OUTCOME, EXCLUDING DATA SENSITIVE TO K AND L SHELL EFFECTS: TEST CASES COMPATIBLE WITH EXPERIMENT AT 0.01 SIGNIFICANCE LEVEL

Test		Penelope 2001	Penelope 2008-2011	EPDL	EPDL ASF	SM	RF	NF	MF	MF ASF	RF ASF
all	Test cases	71	71	71	71	71	71	71	71	71	71
	Pass	19	28	28	18	62	21	26	36	43	40
	Fail	52	43	43	53	9	50	45	35	28	31
	Efficiency	0.27	0.39	0.39	0.35	0.87	0.30	0.37	0.51	0.61	0.56
	Error	± 0.05	± 0.06	± 0.06	± 0.06	± 0.04	± 0.05	± 0.06	± 0.06	± 0.06	± 0.06
$\theta \leq 90^\circ$	Test cases	67	67	67	67	67	67	67	67	67	67
	Pass	19	28	28	25	61	21	26	36	42	38
	Fail	48	39	39	42	6	46	41	31	25	29
	Efficiency	0.28	0.42	0.42	0.37	0.91	0.31	0.39	0.54	0.63	0.57
	Error	± 0.06	± 0.06	± 0.06	± 0.06	± 0.04	± 0.06	± 0.06	± 0.06	± 0.06	± 0.06
$\theta > 90^\circ$	Test cases	17	17	17	17	17	17	17	17	17	17
	Pass	1	1	1	1	11	1	1	0	3	4
	Fail	16	16	16	16	6	16	16	17	14	13
	Efficiency	0.06	0.06	0.06	0.06	0.65	0.06	0.06	< 0.06	0.18	0.24
	Error	± 0.06	± 0.06	± 0.06	± 0.06	± 0.12	± 0.06	± 0.06		± 0.09	± 0.10

TABLE X
GOODNESS-OF-FIT TESTS: TEST CASES COMPATIBLE WITH EXPERIMENT AT 0.05 SIGNIFICANCE LEVEL

Test		Penelope 2001	Penelope 2008-2011	EPDL	EPDL ASF	SM	RF	NF	MF	MF ASF	RF ASF
Kolmogorov Smirnov	Test cases	71	71	71	71	71	71	71	71	71	71
	Pass	67	68	68	61	69	62	67	62	69	64
	Fail	4	3	3	10	2	9	4	9	2	7
	Efficiency	0.94	0.96	0.96	0.86	0.97	0.87	0.94	0.87	0.97	0.90
	Error	± 0.03	± 0.02	± 0.02	± 0.04	± 0.02	± 0.04	± 0.03	± 0.04	± 0.02	± 0.04
Anderson Darling	Pass	68	69	69	62	70	63	69	65	70	63
	Fail	3	2	2	9	1	8	2	6	1	8
	Efficiency	0.96	0.97	0.97	0.87	0.99	0.89	0.97	0.92	0.99	0.89
	Error	± 0.02	± 0.02	± 0.02	± 0.04	± 0.01	± 0.04	± 0.02	± 0.03	± 0.01	± 0.04
	Pass	69	69	69	62	70	66	69	67	70	63
Cramer von Mises	Fail	2	2	2	9	1	5	2	4	1	8
	Efficiency	0.97	0.97	0.97	0.87	0.99	0.93	0.97	0.94	0.99	0.89
	Error	± 0.02	± 0.02	± 0.02	± 0.04	± 0.01	± 0.03	± 0.02	± 0.03	± 0.01	± 0.04

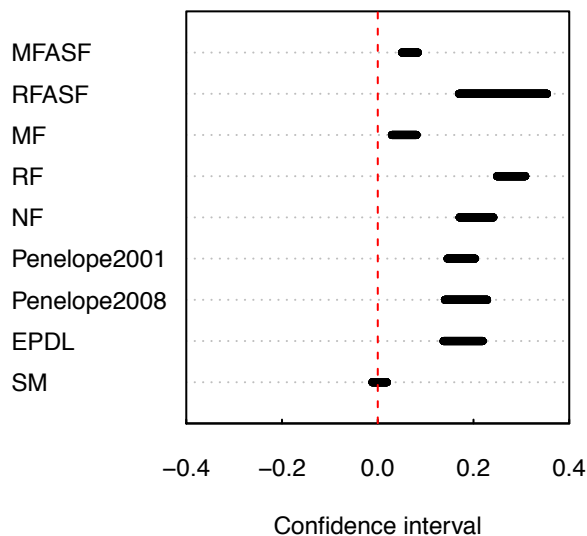


Fig. 6. Confidence intervals for the true mean difference between differential cross sections calculated by Rayleigh scattering simulation models and experimental measurements; the dashed red line identifies the value of zero in the dot chart.

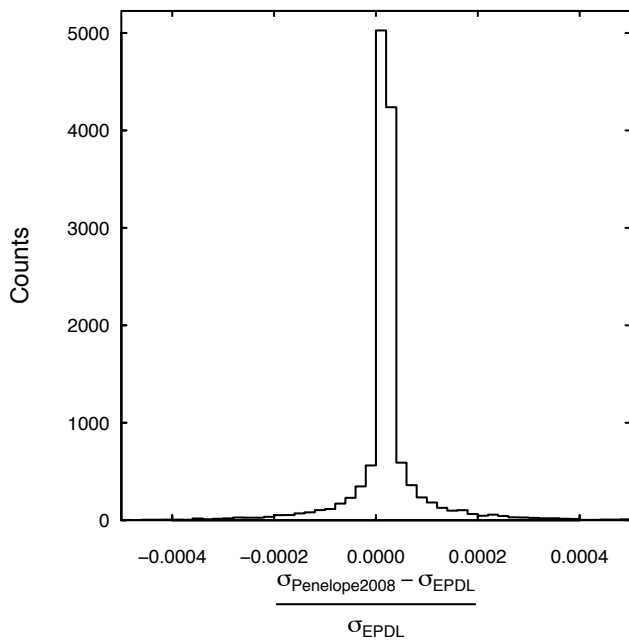


Fig. 7. Relative difference between the total cross sections based on interpolation of Penelope 2008-2011 tabulations derived from EPDL97 and by interpolation of native EPDL97 tabulations as described in [45].

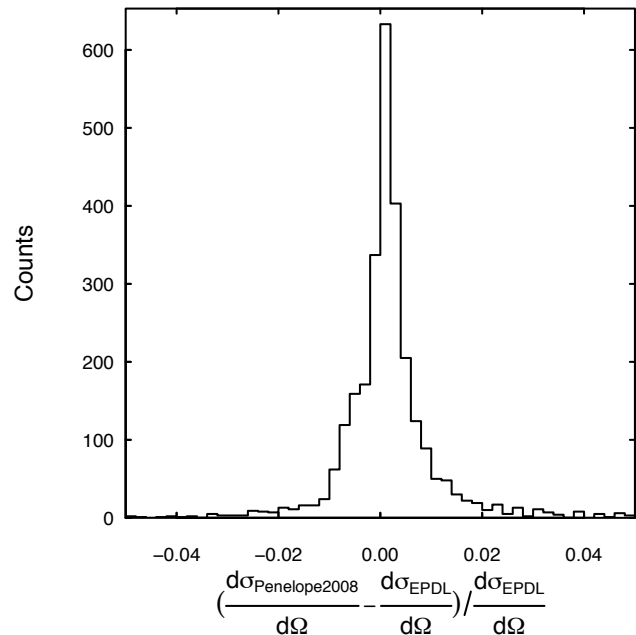


Fig. 8. Relative difference between the differential cross sections calculated based on interpolation of Penelope 2008-2011 tabulated form factors derived from EPDL97 and by interpolation of native EPDL97 tabulations, as described in [45]. The distribution has mean equal to -0.0007 and standard deviation equal to 0.01.

their simulation of photon elastic scattering on EPDL, it is interesting to quantify whether the differential cross sections based on this data library differ significantly in compatibility with experiment from those derived from S-matrix calculations. This analysis is summarized in Table XI, which reports results for the whole data sample, and in Table XII, which excludes data at energies close to K and L shell binding energies; both tables list results calculated over the whole data sample and for scattering angles up to, and above 90° . The hypothesis of statistically equivalent capability to reproduce experimental measurements by the S-matrix simulation model and by the model based on EPDL is rejected at 0.01 level of significance.

Tables XI and XII also report a comparison between the S-matrix model and the model exploiting modified form factors with anomalous scattering factors (MFASF), which exhibits the highest efficiencies in Tables VIII and IX among those based on the form factor approximation. The hypothesis of equivalent accuracy is rejected with 0.01 significance also for the MFASF model over the whole data sample and the subset of data with scattering angles up to 90° , while it is not rejected for the backscattering data sample, although with p-values close to the critical region. A fortiori, simulation models exhibiting lower efficiencies than the MFASF model in Table XI are significantly less accurate than the model based on RTAB S-matrix calculations.

From this analysis one can draw the conclusion that the simulation model based on RTAB tabulations of S-matrix calculations ensures significantly more accurate results than all the other simulation alternatives considered in this study,

including the EPDL data library currently used by several general purpose Monte Carlo systems. The model exploiting modified form factors with anomalous scattering factors is the most accurate among those based on the form factor approximation.

The model based on pristine EPDL97 tabulations of non-relativistic form factors and the Penelope 2008-2011 model, based on modified tabulations derived from EPDL97, produce equivalent differential cross sections: their efficiencies listed in Table XI and XII are identical, despite the small differences visible in Fig. 8. The tabulations of non-relativistic form factors included in RTAB produce slightly less accurate cross sections than the models based on EPDL97, although the differences in efficiencies are compatible within one standard deviation.

The simulation model based on relativistic form factors is less accurate than models exploiting non-relativistic form factors: it has been previously noted [109], [176] that the use of relativistic wavefunctions in the calculation of form factors often produces less accurate results than use of nonrelativistic wavefunctions, although - to the best of our knowledge - the relative efficiency of these two calculation methods at reproducing experimental data has not been yet quantified with statistical methods.

The Penelope 2001 model is less accurate than more recent versions of the code.

The inclusion of anomalous scattering factors in the calculations based on EPDL97 does not contribute to improve compatibility with experiment, while accounting for anomalous scattering improves the compatibility with experiment of calculations exploiting relativistic and modified form factors.

The simplified model in *G4XrayRayleighModel*, which implements elastic scattering from a point-like charge, produces a largely unrealistic description of photon elastic scattering: this is visible, for instance, in Fig. 9, which shows the distribution of the scattering angle of 10 keV photons interacting with carbon generated by this model, compared to the distribution based on S-matrix calculations. Given its evident inadequacy, this model was not included in the statistical analysis for the validation of differential cross sections.

C. Total Cross Sections

Total cross sections calculated by a set of simulation models are shown in Fig. 10 for four representative elements. Some of them are associated with modeling approaches whose capabilities have been evaluated in the previous section regarding differential cross sections: the models based on S-matrix calculations, EPDL97, modified form factors with anomalous scattering factors and Penelope 2001 parameterizations. Others (XCOM, Storm and Israel, Brennan and Cowan), are specific for total cross section calculation only. In addition, the most recent development in the field, Geant4 *G4XrayRayleighModel*, is illustrated in the plots.

The total cross sections calculated by XCOM, Penelope 2001, Storm and Israel, and *G4XrayRayleighModel* appear insensitive to the underlying atomic structure; for photon energies below 10 keV these models overestimate the total

TABLE XI
CONTINGENCY TABLES RELATED TO THE WHOLE DATA SAMPLE

All angles		SM	EPDL
	Pass	55	27
	Fail	16	44
		p-value	
	Fisher test	< 0.001	
	Pearson's χ^2	< 0.001	
	Yates χ^2	< 0.001	
		SM	MFASF
	Pass	55	37
	Fail	16	34
	p-value		
Fisher test	0.003		
Pearson's χ^2	0.002		
Yates χ^2	0.002		
$\theta \leq 90^\circ$		SM	EPDL
	Pass	55	27
	Fail	12	40
		p-value	
	Fisher test	< 0.001	
	Pearson's χ^2	< 0.001	
	Yates χ^2	< 0.001	
		SM	MFASF
	Pass	55	36
	Fail	12	31
	p-value		
Fisher test	< 0.001		
Pearson's χ^2	< 0.001		
Yates χ^2	< 0.001		
$\theta > 90^\circ$		SM	EPDL
	Pass	10	1
	Fail	7	16
		p-value	
	Fisher test	0.002	
	Yates χ^2	0.001	
		SM	MFASF
	Pass	10	2
	Fail	7	15
		p-value	
Fisher test	0.010		
Yates χ^2	0.012		

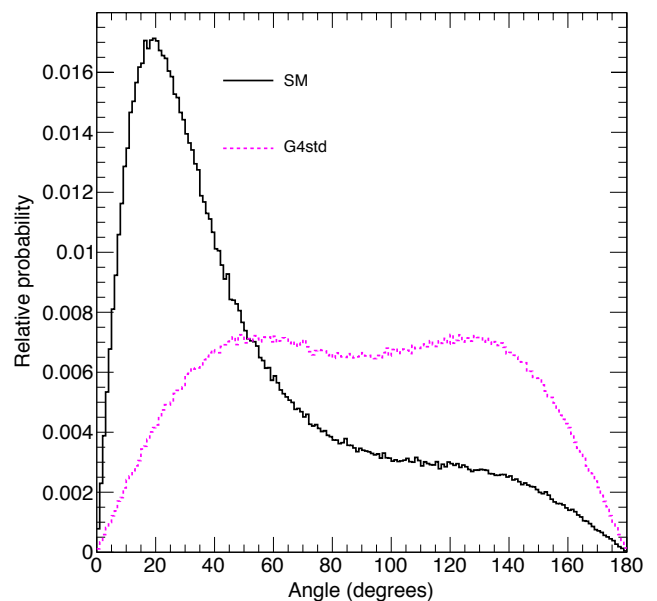


Fig. 9. Probability distribution of the scattering angle of 10 keV photons interacting with carbon generated by *G4XrayRayleighModel* (magenta dashed line) this model, compared to the distribution based on S-matrix calculations (black solid line; both distributions are normalized to 1. The distribution of *G4XrayRayleighModel* corresponds to scattering from a point-like charge.

TABLE XII
CONTINGENCY TABLES EXCLUDING ENERGIES CLOSE TO K AND L SHELL
BINDING ENERGIES

All angles		SM	EPDL
	Pass	62	28
	Fail	9	43
		p-value	
	Fisher test	< 0.001	
	Pearson's χ^2	< 0.001	
	Yates χ^2	< 0.001	
		SM	MFASF
	Pass	62	43
	Fail	9	28
	p-value		
Fisher test	< 0.001		
Pearson's χ^2	< 0.001		
Yates χ^2	< 0.001		
$\theta \leq 90^\circ$		SM	EPDL
	Pass	61	28
	Fail	6	39
		p-value	
	Fisher test	< 0.001	
	Pearson's χ^2	< 0.001	
	Yates χ^2	< 0.001	
		SM	MFASF
	Pass	61	42
	Fail	6	25
	p-value		
Fisher test	< 0.001		
Pearson's χ^2	< 0.001		
Yates χ^2	< 0.001		
$\theta > 90^\circ$		SM	EPDL
	Pass	11	1
	Fail	6	16
		p-value	
	Fisher test	< 0.001	
	Yates χ^2	0.001	
		SM	MFASF
	Pass	11	3
	Fail	6	4
		p-value	
Fisher test	0.013		
Yates χ^2	0.015		

cross section with respect to the S-matrix model, which is the result of the integration of the differential cross sections assessed in section V-B as best reproducing experimental data. The parameterized cross sections by Brennan and Cowan attempt to account for atomic shell effects at low energies, but their results appear largely approximate with respect to S-matrix calculations.

Although in the higher energy end all the calculated cross sections look quite similar on the scale of Fig. 10, differences are visible in Fig. 11, that highlights the behaviour of total cross section models in a region where experimental data are available in the literature [159].

Most of the models shown in Fig. 11 produce qualitatively similar results in that energy range, apart from the interpolation of Storm and Israel's cross sections, the parameterizations by Brennan and Cowan, and *G4XrayRayleighModel*; this model exhibits large discrepancies with respect to Gowda's measurements. The total elastic scattering cross sections calculated by the S-matrix, EPDL and MFASF models are compatible with the measurements in [159] with 0.01 significance; the cross sections based on Storm and Israel's tabulations and calculated by XCOM lie respectively 2.1 and 1.1 standard

deviations away from the experimental values for barium, while they differ from the experimental values of the other three target elements by 3.4 to 5.2 standard deviations. The cross sections calculated by *G4XrayRayleighModel* lie 26 to 41 standard deviations away from the experimental values.

Experimental data from [160] and total cross sections calculated by various simulation models in the energy range between 250 and 700 keV are in Fig. 12 for 9 elements; the experimental errors of the data at 279.2 keV reported in the figure have been scaled by a factor 10 with respect to the values reported in [160], due to the apparent inconsistency discussed in section IV-C. The plots for the other 9 target elements measured in [160] exhibit similar behaviour to those shown in Fig. 12. The source of the data [160], which has not been subject to peer review for publication in a scientific journal, and the concerns about the experimental uncertainties discussed in section IV-C, suggest caution in using these data for quantitative validation of the simulation models; nevertheless, these plots, as well as those for the other 9 measured elements, confirm qualitatively the same conclusions drawn from the analysis of the subset of published data.

Total cross sections based on EPDL97 appear quite similar to those deriving from the integration of S-matrix differential cross sections, whose accuracy has been quantitatively assessed in section V-B. In the energy range between 5 keV and 1.5 MeV, which approximately corresponds to the scope of the validation of differential cross sections documented in section V-B, the Kolmogorov-Smirnov test finds EPDL97 total cross sections compatible with those based on S-matrix calculations for $72\% \pm 5\%$ of the elements, while the total cross sections based on modified form factors with anomalous scattering factors are equivalent to those based on S-matrix for $97\% \pm 2\%$ of the test elements. The significance of these tests is 0.01.

XCOM cross sections are found compatible with those based on S-matrix in $28\% \pm 5\%$ of the test cases; this result can be considered representative also for a set of models (Storm and Israel's, Brennan and Cowan's, Penelope 2001) that exhibit similar characteristics.

Based on these considerations, one can conclude that simulation models based on RTAB tabulated S-matrix results, modified form factors with anomalous scattering factors and EPDL97 are preferable for total cross section calculations to models using Storm and Israel's and XCOM databases, or Penelope 2001 and Brennan and Cowan's parameterizations. It appears also justified to conclude that the cross sections calculated by Geant4 *G4XrayRayleighModel* do not represent a realistic physics model.

D. Nuclear Thomson scattering

The generation of the elastically scattered photon in general purpose Monte Carlo codes only accounts for Rayleigh scattering; RTAB tabulations enable accounting also for nuclear Thomson scattering in the angular distribution of the scattered photon. The contribution due to the nuclear Thomson amplitude is more relevant at higher energies and large angles; as it can be observed in Fig. 2, the inclusion of nuclear

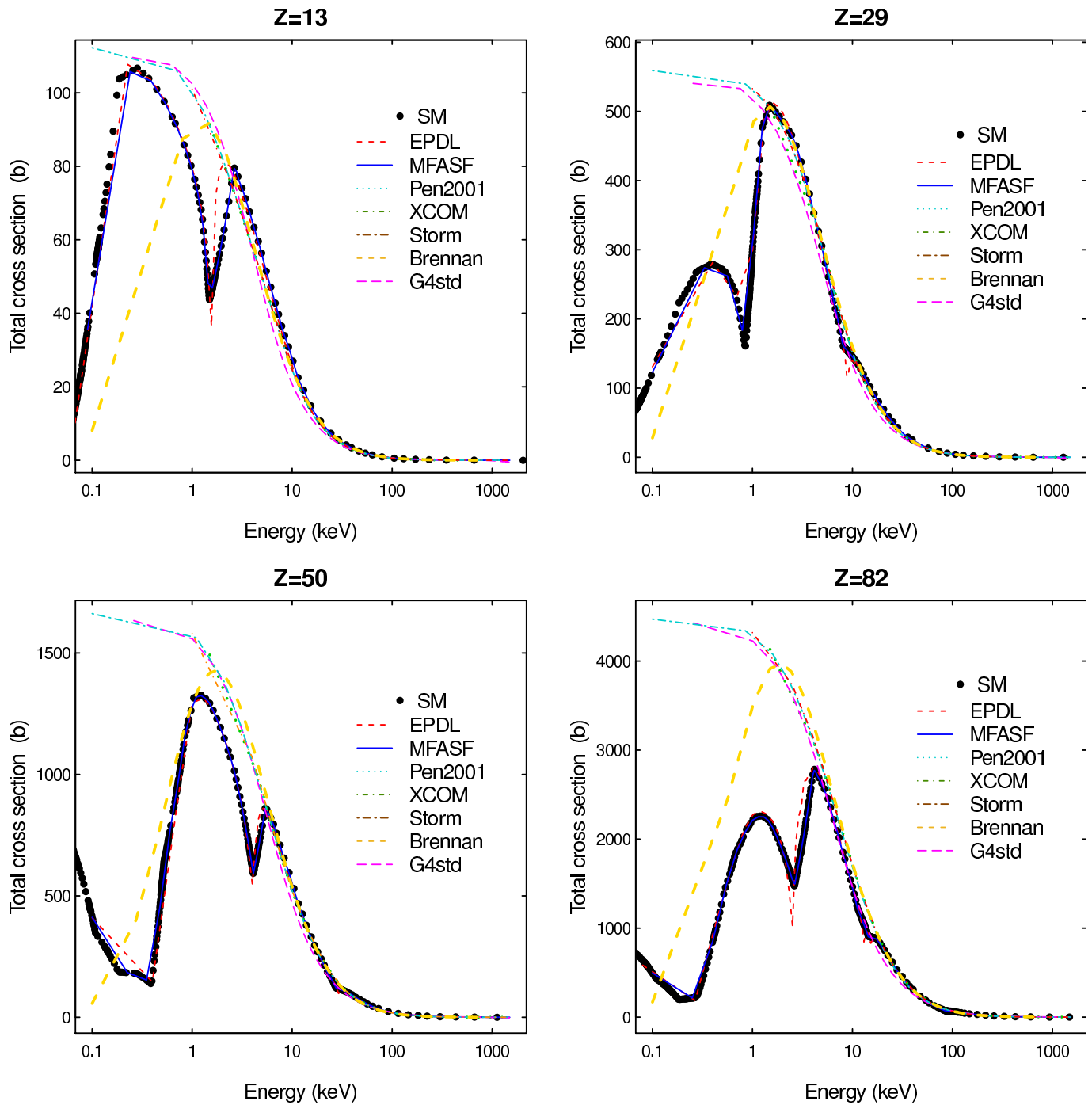


Fig. 10. Total cross section as a function of energy for aluminium, copper, tin and lead: calculations based on S-matrix (SM, black filled circles), EPDL (red dashed line), modified form factors with anomalous scattering factors MFASF (blue solid line), XCOM (green dotted line), Storm and Israel (brown dotted-dashed line), Penelope 2001 (turquoise double-dashed line), Brennan and Cowan (yellow dashed line) and *G4XrayRayleighModel* (G4std, magenta long-dashed line).

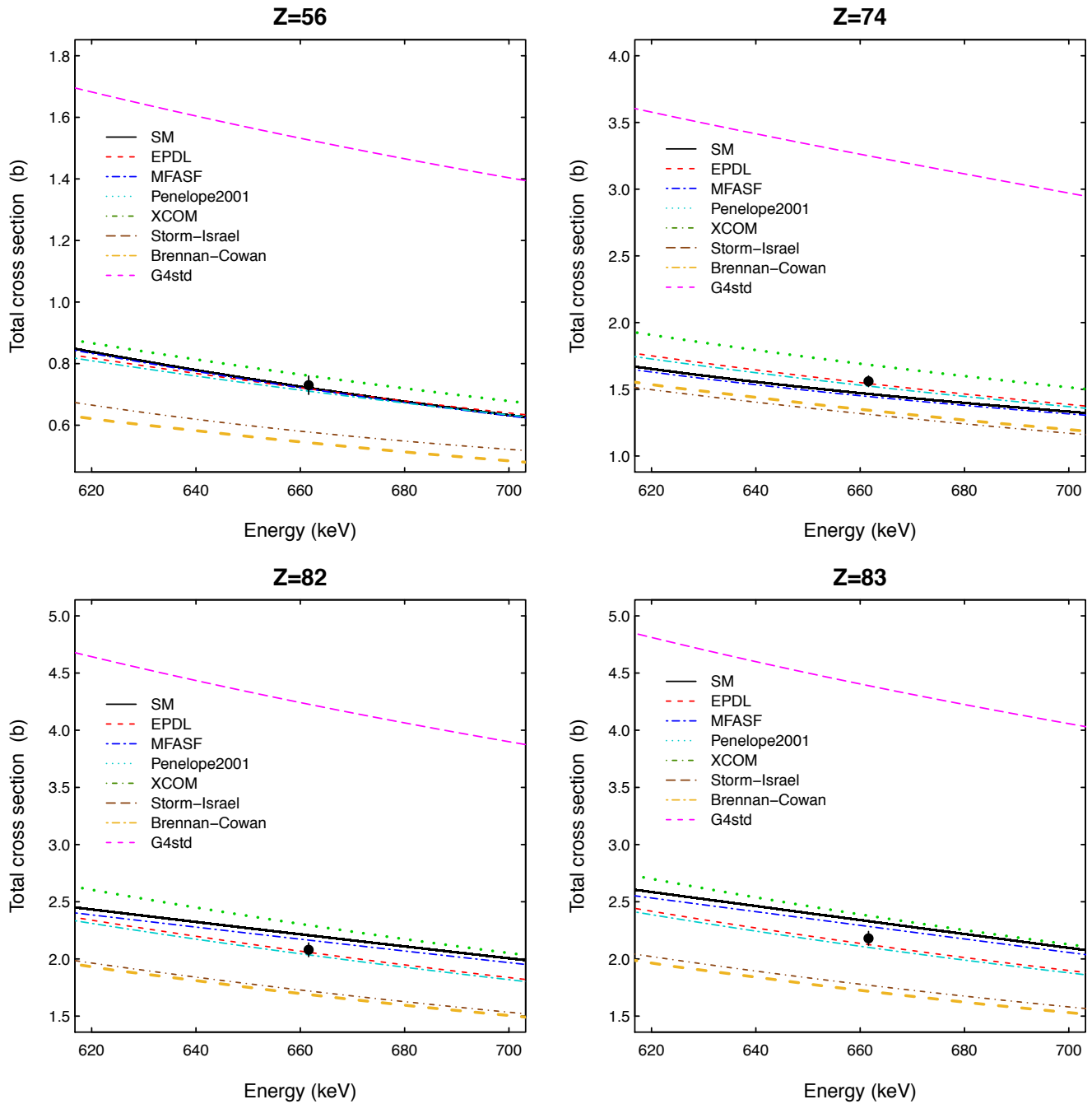


Fig. 11. Total cross section as a function of energy for barium, tungsten, lead and bismuth: calculations based on S-matrix (SM, black solid line), EPDL (red dashed line), modified form factors with anomalous scattering factors MFASF (blue double-dashed line), XCOM (green dotted line), Storm and Israel (brown dotted-dashed line), Penelope 2001 (turquoise double-dashed line), Brennan and Cowan (yellow dashed line) and *G4XrayRayleighModel* (G4std, magenta long-dashed line), and experimental data (black circles) from [159]. In some plots the experimental errors are smaller than the symbol size.

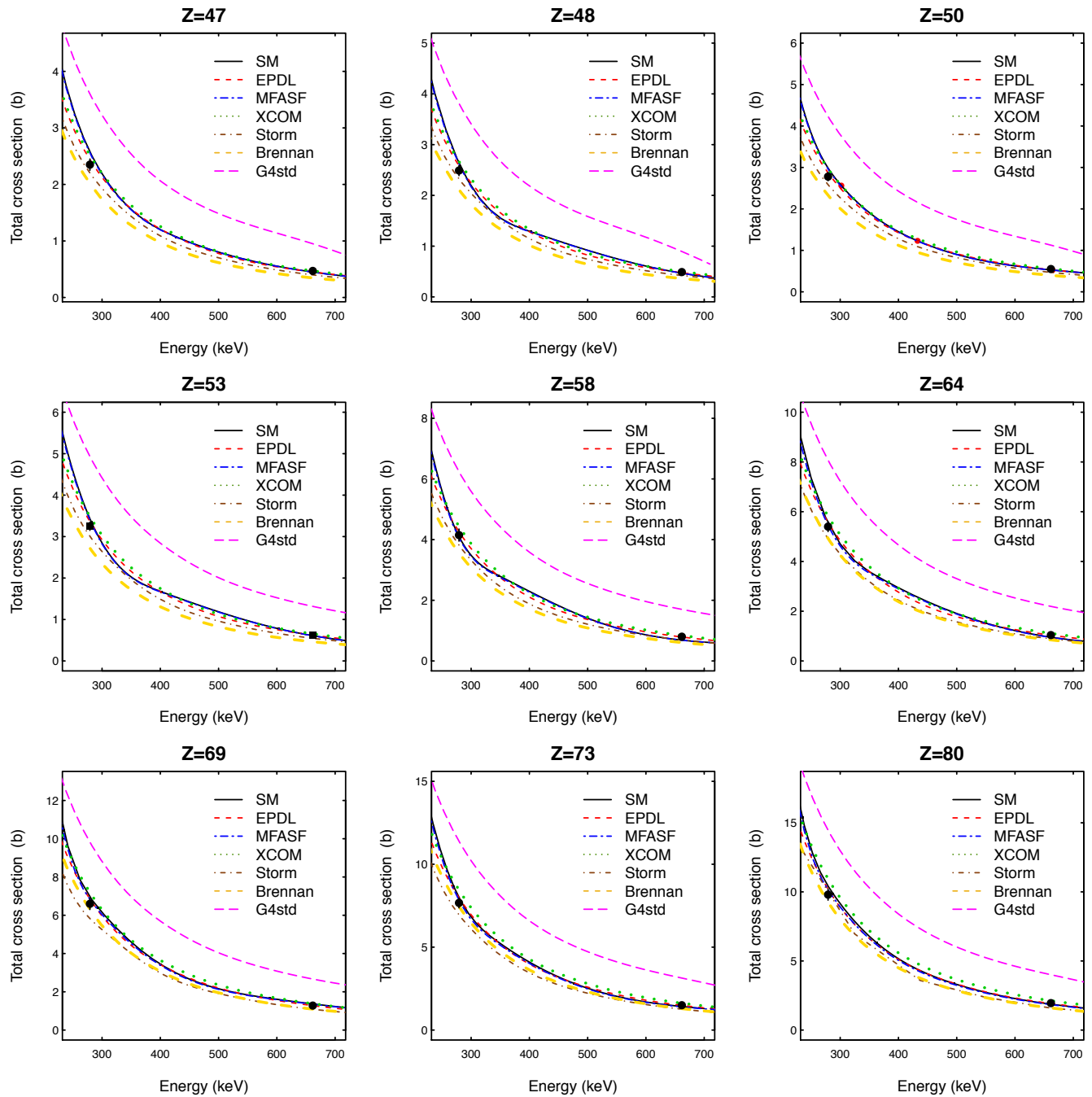


Fig. 12. Total cross section as a function of energy for silver, cadmium, tin, iodine, cerium, gadolinium, thulium, tantalum and mercury: calculations based on S-matrix (SM, black solid line), EPDL (red dashed line), modified form factors with anomalous scattering factors MFASF (blue double-dashed line), XCOM (green dotted line) and Storm and Israel (brown dotted-dashed line), Brennan and Cowan (yellow dashed line) and *G4XrayRayleighScatteringModel* (G4std, magenta long-dashed line) and experimental measurements from [160] (black dots). The Penelope 2001 model, not shown for better clarity of the plots, exhibits similar behaviour to XCOM cross sections. In some plots the experimental errors are smaller than the symbol size.

Thomson scattering in the simulation has significant effects on the correct estimate of photon backscattering.

The effect of accounting for the nuclear Thomson amplitude on the accuracy of the simulation is summarized in Table XIII. The results concern the comparison of differential cross sections with experiment, and consist of the efficiency for two variants of the S-matrix model, respectively accounting for Rayleigh scattering and Nuclear Thomson scattering, or neglecting the latter; they are reported in three test configurations, concerning the whole data sample and the data respectively below and above 90° . In all the configurations the inclusion of nuclear Thomson scattering contributes to improving the accuracy of the simulation.

TABLE XIII

EFFICIENCIES FOR DIFFERENTIAL CROSS SECTIONS BASED ON S-MATRIX CALCULATIONS ACCOUNTING FOR RAYLEIGH SCATTERING ONLY OR INCLUDING ALSO NUCLEAR THOMSON SCATTERING

	SM	SM
	Rayleigh	Rayleigh + Nuclear Thomson
all	0.72 ± 0.05	0.77 ± 0.05
$\theta < 90^\circ$	0.76 ± 0.05	0.82 ± 0.05
$\theta > 90^\circ$	0.35 ± 0.12	0.59 ± 0.12

E. Simulation at the electronvolt scale

Microdosimetry and nanodosimetry simulation requires the capability of modeling particle interactions with matter down to the scale of a few electronvolts. EPDL97 includes tabulations of Rayleigh total cross sections down to 1 eV, nevertheless, its documentation warns about using the data below 100 eV for photon transport calculations, since “the uncertainty in the data rapidly increases with decreasing energy” [19].

A qualitative comparison of EPDL97 total Rayleigh scattering cross sections and experimental data [177]–[190] for rare gases, hydrogen and atomic nitrogen at energies between 1.8 and 11.2 eV is illustrated in Fig. 13. Although one can observe some resemblance between EPDL97 calculations and experimental cross section measurements in some of the plots and large discrepancies in other ones, a quantitative appraisal of the accuracy of EPDL97 is not realistic due to the scarcity of experimental data, their inconsistencies and possible systematic effects introduced by normalization procedures applied to some of the experimental data.

Further experimental measurements would be needed for a thorough assessment of simulation models meant for microdosimetry simulation.

F. Interpolation algorithms

Simulation models based on data tabulations calculate the physical quantities needed in the course of particle transport by interpolation over the tabulated values. This method has the advantage of avoiding the computation of complex analytical formulae in the course of simulation execution; nevertheless, interpolation methods themselves could be computationally expensive, especially if they involve calls to library functions

(e.g. the calculation of logarithms) rather than elementary arithmetic operations only.

EPDL documentation recommends double-logarithmic interpolation over the tabulated data; this prescription has been adopted for the related simulation models [45]. The same interpolation method has been used also for the other models based on form factor tabulations to ensure a uniform treatment.

The use of S-matrix tabulations requires two-dimensional interpolation over energy and angle for any given target atomic number. Three interpolation algorithms have been evaluated, considering both the resulting physics accuracy and their computational performance: linear and logarithmic interpolation, and a simplified interpolation method described in [22], which utilizes scaling factors related to MFASF tabulations. Table XIV summarizes the efficiency at producing results consistent with experiment associated with various interpolation method; they concern the Rayleigh scattering amplitude only, but the conclusions hold also for other amplitudes. The logarithmic interpolation algorithm determines differential cross sections that are compatible with experiment at 0.01 level of significance in a larger number of test cases; nevertheless, the efficiencies resulting from the three algorithms are compatible within one standard deviation.

Although less accurate than logarithmic interpolation, linear interpolation of S-matrix tabulations produces estimates in better agreement with experiment than models based on the form factor approximation; therefore, if computational performance is a concern, one can opt for linearly interpolating S-matrix tabulations, still preserving the superior accuracy of this model with respect to other physics approximations despite some degradation with respect to logarithmic interpolation.

Programming techniques for performance optimization [191]–[193] and more refined interpolation methods than those discussed in this paper can be applied for efficient tabulated data management; their in-depth discussion is outside the scope of this paper.

TABLE XIV

EFFECT OF INTERPOLATION ALGORITHMS

	SM	SM	SM
	linear	logarithmic	simplified
Test cases	71	71	71
Pass	49	51	48
Fail	22	20	23
Efficiency	0.69	0.72	0.68
Error	± 0.05	± 0.05	± 0.05

G. Computational performance

Computational performance is an important issue in assessing whether a physics model is suitable for Monte Carlo particle transport, and in optimizing the selection of physics models for the simulation of a given experimental scenario, when multiple options are available.

The validation analysis documented in section V-B has identified the simulation model based on RTAB tabulations of second order S-matrix calculations as the most accurate at reproducing experimental measurements of elastic scattering differential cross sections, i.e. at determining the actual outcome

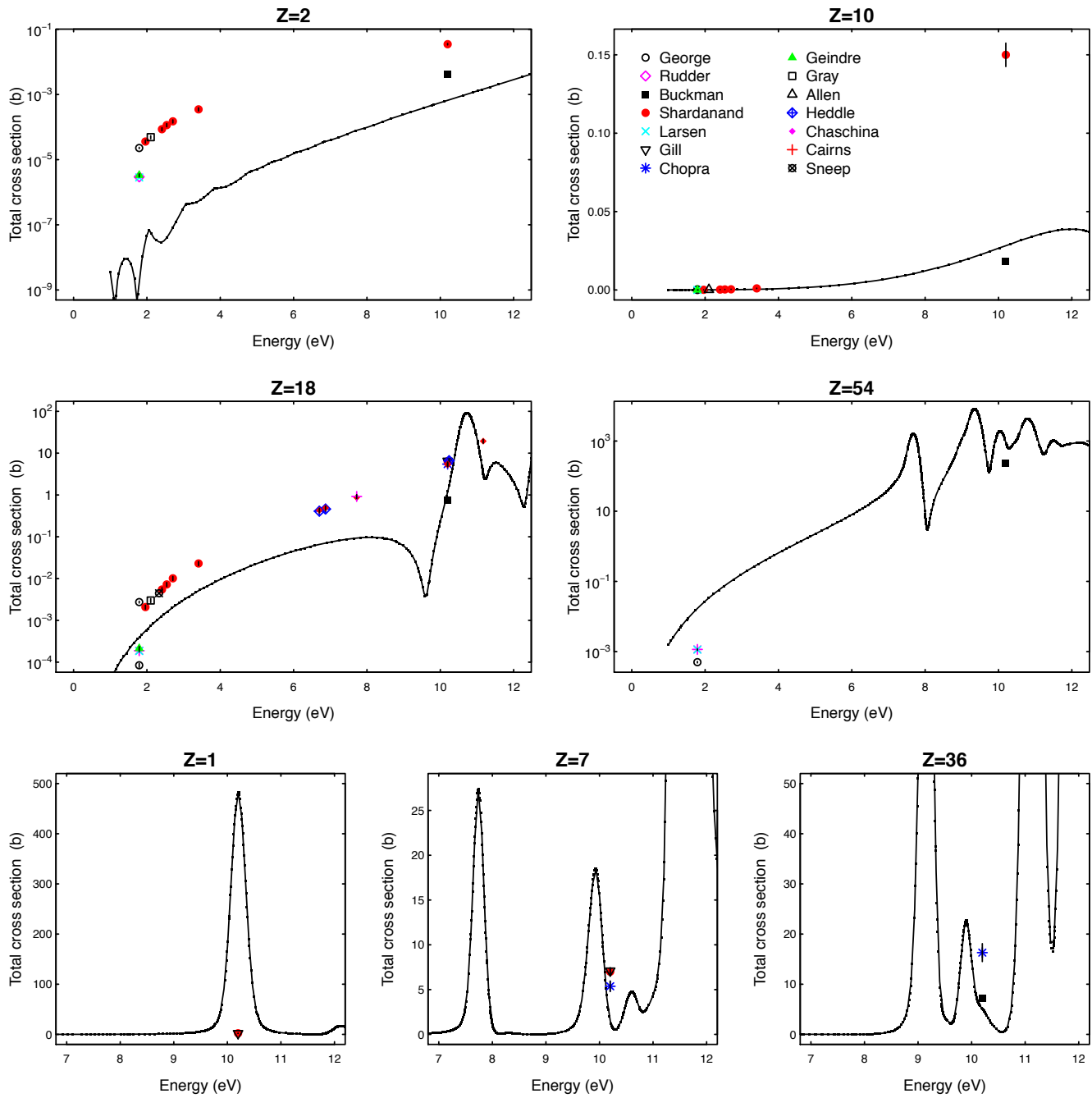


Fig. 13. Total cross section as a function of energy for rare gases (helium, neon, argon, krypton and xenon), hydrogen and nitrogen in the electronvolt energy range: EPDL (black solid line), and experimental measurements [177]–[190]. The legend reported in the plot for neon is pertinent to all the plots; the experimental data are identified by the name of the first author of the corresponding publication. Please note that the plots for helium, argon and xenon are in logarithmic scale on the vertical axis, while the others are in linear scale. The error bars that are not visible in the plots are smaller than the symbol size.

of the scattering process. Nevertheless, the use of S-matrix tabulations in particle transport requires more complex operations than models based on the form factor approximation, since it implies the management of two-dimensional tabulations (over a grid of energies and angles) and the development of an ad hoc algorithm to sample the direction of the scattered photon, replacing the sampling algorithms that are currently established to deal with the form factor approximation. The comparative evaluation of its computational performance with respect to models based on the form factor approximation is relevant to determine whether this modeling approach, that has not yet been exploited in Monte Carlo codes, is practically usable in that context.

From another standpoint, less accurate models, for instance based on parameterizations or neglecting some physical features, could be justified for inclusion in a simulation system, if they provide significantly faster computational performance than more accurate alternatives.

The analysis addresses various issues related to how features specific to different photon elastic scattering modeling approaches and software algorithms affect the computational performance of the simulation. Evaluations of computational performance are necessarily specific to a given Monte Carlo code, computing platform and test case; the results reported here concern test cases using the Geant4 toolkit, and have been obtained on an AMD 2.4 GHz 2-core processor computer with Scientific Linux 5 operating system and the gcc 4.1.2 compiler.

From a computational perspective, one can distinguish two methods of total cross section calculation as a function of energy: either by interpolation of tabulated values, or by means of analytical formulae. In the context of Geant4 the former method is used by the models based on EPDL97, while the latter is used by *G4XrayRayleighModel* and by the model derived from Penelope 2001. Total cross sections based on S-matrix calculations are computed by interpolation of tabulations as well; therefore, in computational terms, they do not differ from calculations currently based on EPDL97.

Two test cases have been evaluated as representative of the computational burden associated with either method; they concern the average time to calculate one million total cross sections, for atomic number between 1 and 99, and photon energy between 250 eV and 50 keV. The computation time is 0.277 ± 0.019 seconds for a model based on the interpolation of EPDL97, and 0.332 ± 0.007 seconds for the analytical algorithm implemented in *G4XrayRayleighModel*; it appears independent from the photon energy. The hypothesis of equivalent computational impact of the two calculation methods is rejected 99% confidence level in this test case, i.e. the calculation of total cross sections based on the interpolation of EPDL97 is significantly faster than the calculation performed by the simplified *G4XrayRayleighModel*. However, this result should not be generalized to the computational equivalence of interpolation and analytical algorithms in absolute terms, since the relative performance of these calculation methods depends on the computational complexity of the analytically formulae and on the characteristics of the interpolation algorithms subject to test.

Nevertheless, the computational impact of total cross section

calculation methods on Monte Carlo simulation is marginal, since in general it affects the computational performance only in the initialization phase of the simulation: for instance, in Geant4 atomic total cross sections are calculated at initialization in the process of building mean free path tabulations for each material present in the geometrical model of the experimental set-up, which are then used in the course of particle transport.

Two issues contribute to the computational performance of the actual photon scattering simulation: the calculation of the physical distribution to sample the scattering angle, and the sampling algorithm. The calculation of the distribution to sample can occur by interpolation of tabulated values or through an analytical formula.

The computational performance of a set of representative methods for the generation of the elastically scattered photon has been analyzed on a test case consisting of one million primary photons with energy between 250 eV and 1 MeV, which are only subject to elastic scattering as possible interaction with matter. The Geant4-based application developed for this test can be configured to use any of the existing Rayleigh scattering options in Geant4 9.5 or the newly developed software described in this paper, namely elastic scattering based on S-matrix calculations; it provides options for elemental targets with atomic number between 1 and 99.

The results of this test are illustrated in Fig. 14, which report the average time to simulate one million events as a function of photon energy for two representative test cases (carbon and lead as targets); the plotted values are scaled to the time needed to simulate one million events with 10 keV primary photons and copper as a target.

The computational performance of physics models based on the form factor approximation appears independent from the way the sampling distribution is calculated, but is strongly affected by the efficiency of the sampling algorithm. It is comparable for the Penelope 2001 and 2008 scattering implementations, which adopt the same sampling algorithm (based on inverse transform adaptive sampling [48]), but calculate the sampling distribution respectively from an analytical formula and by interpolation. It exhibits large differences for the Geant4 Penelope 2008 and Livermore implementations, which both interpolate EPDL97 tabulations, but use different sampling algorithms (acceptance-rejection sampling for the Livermore model, a form of inverse transform sampling for Penelope [40]). The inefficiency of the acceptance-rejection algorithm shows a strong dependence on the photon energy, which severely affects the computational performance of the elastic scattering simulation above approximately a few tens keV.

The simplified physics model implemented in *G4XrayRayleighModel* does not exhibit any significant computational advantage with respect to the interpolation of EPDL97 with inverse transform sampling, which is available in Geant4 through the reengineered Penelope 2008 model.

The generation of photon elastic scattering based on S-matrix calculations is approximately a factor two slower than the method based on the form factor approximation exploiting inverse transform sampling, which, among the test cases illus-

trated in Figs. 14, is represented by the reengineered Penelope 2008 model: the difference is due to performing interpolation over bi-dimensional tabulations rather than one-dimensional interpolation. The final state generation model based on S-matrix calculations exploits the inverse transform algorithm to sample the scattering angle, similarly to the Penelope models; thanks to its more efficient sampling algorithm, it is significantly faster than the model based on EPDL97 form factors currently implemented in Geant4, which utilizes an acceptance-rejection sampling algorithm.

A factor two degradation in the computational performance of photon elastic scattering simulation can be considered an acceptable compromise for most experimental applications requiring accurate simulation of photon interactions, given the superior physical performance of this model demonstrated by the validation documented in section V-B.

It should be stressed that the degradation of performance discussed in this context is limited to photon elastic scattering, while in experimental practice other types of photon interactions, and of their secondary products, are usually activated in the simulation: the factor two penalty in computational performance represents an upper limit, which corresponds to applications only involving photon elastic scattering. The relative impact of photon elastic scattering on the overall computational performance cannot be quantified in general terms, since it depends on many physical and user parameters specific to a given experimental scenario: some factors affecting the computational speed of a simulation are the energy of the particles involved, the materials of the experimental set-up, the physics processes and models activated in the simulation, secondary production thresholds and other user cuts, the complexity of the geometrical configuration, and the characteristics of the user application software, but this enumeration is not intended to be exhaustive.

A policy class for final state generation has been developed in the context of this study, which can exploit any form factor tabulation and uses an inverse transform algorithm to sample the photon scattering angle. This class provides optimal computational performance, while it substantially improves simulation accuracy with respect to the Penelope 2008 model, still in the form factor approximation, by using modified form factors with angle independent anomalous scattering factors.

VI. CONCLUSION

An extensive set of models for the simulation of photon elastic scattering has been quantitatively evaluated regarding their accuracy at reproducing experimental measurements and their computational performance.

The analysis has identified the simulation of photon elastic scattering based on second order S-matrix calculations tabulated in RTAB as the state-of-the-art. This model, that accounts for Rayleigh scattering and nuclear Thomson scattering, represents approximately a factor two improvement in compatibility with experiment with respect to the Rayleigh scattering models currently available in Geant4 and in other general purpose Monte Carlo codes. The inclusion of nuclear Thomson scattering is relevant especially at higher energies

and for backscattering. Complementary evaluation of the computational performance has demonstrated that photon elastic scattering simulation based on S-matrix calculations is practically feasible in a general purpose Monte Carlo system, despite its greater computational complexity than models based on the form factor approximation currently in use.

The results of the analysis hint that the accuracy of simulation based on S-matrix calculations could be further improved by optimizing the tabulation grid of RTAB for more precise interpolation in areas that are sensitive to the underlying atomic structure. Nevertheless, the production of an extended data library of second order S-matrix calculations would require significant computational investment and the collaboration of expert theoreticians.

If one prefers to base the simulation of Rayleigh scattering on the form factor approach to avoid more complex computations required by the S-matrix model, modified form factors with anomalous scattering factors (MFASF) appear the preferable choice among the various form factor options examined in this paper, although they result in degraded simulation accuracy with respect to the state-of-the-art model based on S-matrix calculations. The choice of the method to sample the direction of the scattered photon is critical for computational performance: inverse transform sampling is preferable to acceptance-rejection.

Relativistic form factors result in worse accuracy than other form factor options (non-relativistic and modified); therefore their use in simulation models is not encouraged.

Anomalous scattering factors calculated in the RTAB theoretical environment contribute to improve the accuracy of cross sections based on modified and relativistic form factors, while the anomalous scattering factors included in EPDL97 do not improve the results based on this data library.

Total and differential cross sections calculated by interpolation of pristine EPDL97 tabulations, and by the reengineered code and reprocessed EPDL97 tabulations originating from Penelope 2008 produce equivalent physics results. The maintenance in Geant4 of two implementations that conform to the same software design scheme and produce equivalent physics outcome appears redundant.

The total cross sections calculated by the Penelope 2001 model neglect the underlying atomic structure in the low energy range, and the differential cross sections exhibit significantly worse accuracy than other models based on the form factor approximation: the maintenance of the Penelope 2001 model in Geant4 does not appear physically justified.

Total cross sections calculated by XCOM, Storm and Israel, and Brennan and Cowan look qualitatively similar; they exhibit relatively limited differences with respect to cross sections based on EPDL97 and on S-matrix calculations above approximately 10 keV, but they appear largely deficient at reproducing effects close to absorption edges.

The total cross sections calculated by Geant4 *G4XrayRayleighModel* are insensitive to the atomic structure at low energies, and largely inconsistent with experimental data in the energy range of a few hundred keV. The scattering angle distribution produced by this model corresponds to Thomson scattering by a point-like charge, which is an

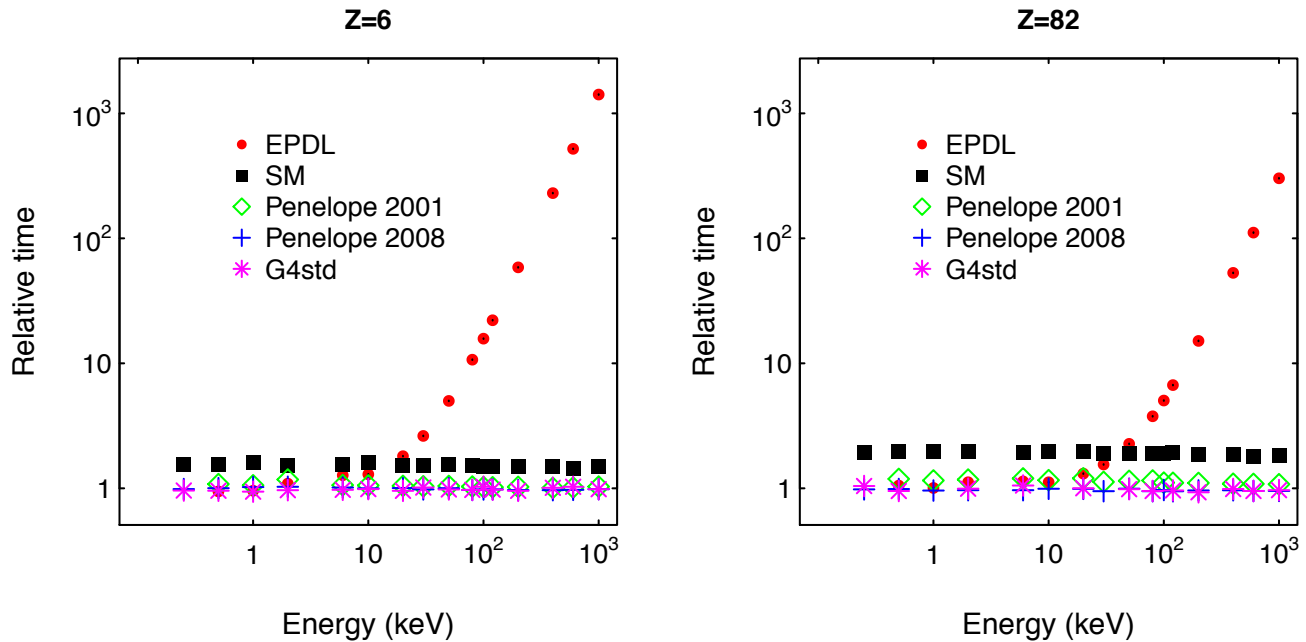


Fig. 14. Time spent to simulate one million photon elastic scatterings with carbon (left) and lead (right), as a function of photon energy with current Geant4 Rayleigh scattering implementations and with the new model based on S-matrix calculations: reengineered Penelope 2001 and 2008 models (respectively green diamond and blue cross), EPDL-based “Livermore” model (red circles), *G4XrayRayleighModel* (magenta asterisk) and S-matrix model (SM, black squares). The timing is expressed in relative units with respect to the time spent to simulate one million scatterings with copper at 10 keV using the Geant4 model reengineered from Penelope 2008. The error bars are not visible in the plot, as they are smaller than the symbol size.

unrealistic description of photon elastic scattering. This model does not exhibit any computational advantage with respect to more accurate models currently available in Geant4. Further maintenance of this model in Geant4 should be seriously considered.

The policy-based software design adopted in this study for the simulation of photon elastic scattering has played a key role in ensuring versatility of modeling, at the same time greatly facilitating the verification and validation process due to minimization of the dependencies of basic physics code on other parts of Geant4. This finding is relevant in view of future design evolutions of the Geant4 toolkit to improve its reliability and to reduce the efforts invested for quality assurance and maintenance.

The software for the simulation of photon elastic scattering developed for this study will be proposed for release in a forthcoming Geant4 version, following the publication of this paper, to improve Geant4 capabilities in this physics domain.

ACKNOWLEDGMENT

The authors are grateful to Lynn Kissel for valuable information and advice, and to Andrew Buckley for proofreading the manuscript and useful comments.

The CERN Library, in particular Tullio Basaglia, has provided helpful assistance and essential reference material for this study.

REFERENCES

- [1] R. Cesareo, A. L. Hanson, G. E. Gigante, L. J. Pedraza, and S. Q. G. Mahtabally, “Interaction of keV photons with matter and new applications”, *Phys. Rep.*, vol. 213, no. 3, pp. 117-178, 1992.
- [2] J. H. Hubbell, “Review and history of photon cross section calculations”, *Phys. Med. Biol.*, vol. 51, pp. R245-R262, 2006.
- [3] P. P. Kane, L. Kissel, R. H. Pratt, and S. C. Roy, “Elastic scattering of γ -rays and X-rays by atoms”, *Phys. Rep.*, vol. 140, no. 2, pp. 75-159, 1986.
- [4] S. C. Roy, L. Kissel, and R. H. Pratt, “Elastic scattering of photons”, *Rad. Phys. Chem.*, vol. 56, pp. 3-26, 1999.
- [5] D. A. Bradley, O. D. Gonçalves, and P. P. Kane, “Measurements of photon-atom elastic scattering cross-sections in the photon energy range 1 keV to 4 MeV”, *Rad. Phys. Chem.*, vol. 56, pp. 125-150, 1999.
- [6] K. Amako et al., “Comparison of Geant4 electromagnetic physics models against the NIST reference data”, *IEEE Trans. Nucl. Sci.*, vol. 52, no. 4, pp. 910-918, 2005.
- [7] T. G. Trucano, L. P. Swiler, T. Igusa, W. L. Oberkampf, and M. Pilch, “Calibration, validation, and sensitivity analysis: Whats what”, *Reliab. Eng. Syst. Safety*, vol. 91, no. 10-11, pp. 1331-1357, 2006.
- [8] G. A. P. Cirrone, G. Cuttone, F. Di Rosa, L. Pandola, F. Romano, and Q. Zhang, “Validation of the Geant4 electromagnetic photon cross-sections for elements and compounds”, *Nucl. Instr. Meth. A*, vol. 618, pp. 315-322, 2010.
- [9] S. Agostinelli et al., “Geant4 - a simulation toolkit” *Nucl. Instrum. Meth. A*, vol. 506, no. 3, pp. 250-303, 2003.
- [10] J. Allison et al., “Geant4 Developments and Applications” *IEEE Trans. Nucl. Sci.*, vol. 53, no. 1, pp. 270-278, 2006.
- [11] R. H. Pratt, L. Kissel, and P. M. Bergstrom, “New relativistic S-matrix results for scattering beyond the usual anomalous factors/beyond impulse approximation”, in *Resonant Anomalous X-ray Scattering - Theory and Applications*, Elsevier Science, Amsterdam, pp. 9-33, 1994.
- [12] N. A. Dyson, “X-rays in Atomic and Nuclear Physics”, Cambridge University Press, 2nd ed., pp. 215-219, 1990.
- [13] J. H. Hubbell, W. J. Viegele, E. A. Briggs, R. T. Brown, D. T. Cromer, and R. J. Howerton, . “Atomic form factors, incoherent scattering functions, and photon scattering cross sections”, *J. Phys. Chem. Ref. Data*, vol. 4, pp. 471-538, 1975.
- [14] J. H. Hubbell and I. Overbø, “Relativistic atomic form factors and photon coherent scattering cross sections”, *J. Phys. Chem. Ref. Data*, vol. 8, pp. 69-105, 1979.
- [15] D. Schaupp, M. Schumacher, F. Smend, P. Rullhusen, and J. H. Hubbell, “Small angle Rayleigh scattering of photons at high energies:

- Tabulation of relativistic HFS modified atomic form factors”, *J. Phys. Chem. Ref. Data*, vol. 12, pp. 467-508, 1983.
- [16] G. E. Brown, R. E. Peierls, J. B. Woodward, “The coherent scattering of γ -rays by K-electrons in heavy atoms”, *Proc. R. Soc. London A*, vol. 227, no. 1168, pp. 51-58, 1955.
- [17] L. Kissel and R. H. Pratt, “Rayleigh scattering - elastic photon scattering by bound electrons”, in *Atomic Inner-shell Physics*, Plenum Press, New York, pp. 465-498, 1985.
- [18] L. Kissel, B. Zhou, S. C. Roy, S. K. Sen Gupta, and R. H. Pratt, “The validity of form factor, modified form factor and anomalous scattering factor approximations in elastic scattering calculations” *Acta Cryst. A*, vol. 51, pp. 271-288, 1995.
- [19] D. Cullen et al., “EPDL97, the Evaluated Photon Data Library”, Lawrence Livermore National Laboratory Report UCRL-50400, Vol. 6, Rev. 5, 1997.
- [20] M. B. Chadwick et al., “ENDF/B-VII.1 Nuclear Data for Science and Technology: Cross Sections, Covariances, Fission Product Yields and Decay Data”, *Nucl. Data Sheets*, vol. 112, no. 12, pp. 2887-3152, 2011.
- [21] D. E. Cullen, “Program SCATMAN: A Code Designed to Calculate Photon Coherent Scattering Anomalous Scattering Factors and Cross Sections”, Lawrence Livermore National Laboratory UCRL-ID-103422 Report, 1989.
- [22] L. Kissel, “RTAB: the Rayleigh scattering database”, *Radiat. Phys. Chem.*, vol. 59, pp. 185-200, 2000.
- [23] L. R. M. Morin, “Molecular Form Factors and Photon Coherent Scattering Cross Sections of Water”, *J. Phys. Chem. Ref. Data*, vol. 11, pp. 1091-1098, 1982.
- [24] H. Hirayama, Y. Namito, A. F. Bielajew, S. J. Wilderman, and W. R. Nelson, “The EGS5 Code System”, SLAC-R-730 Report, Stanford, CA, 2006.
- [25] W. R. Nelson, H. Hirayama, and D. W. O. Rogers, “The EGS4 Code System”, SLAC-265 Report, Stanford, CA, 1985.
- [26] E. Storm and H. I. Israel, “Photon cross sections from 1 keV to 100 MeV for elements Z=1 to Z=100”, *Atom. Data Nucl. Data Tables*, vol. 7, pp. 565-681, 1970.
- [27] H. P. Hanson, F. Herman, J. D. Lea, and S. Skillman, “HFS Atomic Scattering Factors”, *Acta Cryst.*, vol. 17, pp. 1040-1044, 1964.
- [28] I. Kawrakow, E. Mainegra-Hing, D.W.O. Rogers, F. Tessier and B.R.B. Walters, “The EGSnrc Code System: Monte Carlo Simulation of Electron and Photon Transport NRCC PIRS-701, 5th printing, 2010.
- [29] M. J. Berger et al., “XCOM: Photon Cross section Database (version 1.5)”, National Institute of Standards and Technology, Gaithersburg, MD, 2010. [Online] Available: <http://physics.nist.gov/xcom>.
- [30] S. M. Seltzer, “Electron-Photon Monte Carlo Calculations: The ETRAN Code”, *Appl. Radiat. Isot.*, vol. 42, no. 10, pp. 917-941, 1991.
- [31] G. Battistoni et al., “The FLUKA code: description and benchmarking”, *AIP Conf. Proc.*, vol. 896, pp. 31-49, 2007.
- [32] A. Ferrari et al., “Fluka: a multi-particle transport code”, Report CERN-2005-010, INFN/TC-05/11, SLAC-R-773, Geneva, Oct. 2005.
- [33] B. C. Franke, R. P. Kensek and T. W. Laub, “ITS5 theory manual”, rev. 1.2, Sandia Natl. Lab. Report SAND2004-4782, Albuquerque, 2004.
- [34] X-5 Monte Carlo Team, “MCNP – A General Monte Carlo N-Particle Transport Code, Version 5”, Los Alamos National Laboratory Report LA-UR-03-1987, 2003, revised 2008.
- [35] J. S. Hendricks et al., “MCNPX, Version 2.6.0”, Los Alamos National Laboratory Report LA-UR-06-7991, 2008.
- [36] D. E. Cullen et al., “Tables and Graphs of Photon Interaction Cross Sections from 10 eV to 100 GeV Derived from the LLNL Evaluated Photon Data Library (EPDL)”, Lawrence Livermore National Laboratory Report UCRL-50400, Vol. 6, Rev. 4, 1989.
- [37] D. Garber Ed. , “ENDF/B Summary Documentation”, BNL-17541, 1975.
- [38] D. B. Pelowitz et al., “MCNPX 2.7.E Extensions”, Los Alamos National Laboratory Report LA-UR-11-01502, 2011.
- [39] J. Baro, J. Sempau, J. M. Fernández-Varea, and F. Salvat, “PENELOPE, an algorithm for Monte Carlo simulation of the penetration and energy loss of electrons and positrons in matter”, *Nucl. Instrum. Meth. B*, vol. 100, no. 1, pp. 31-46, 1995.
- [40] F. Salvat, J.M. Fernandez-Varea, and J. Sempau, “Penelope - A code system for Monte Carlo simulation of electron and photon transport”, Proc. Workshop NEA 6416, 2008.
- [41] F. Salvat, J.M. Fernandez-Varea, and J. Sempau, “Penelope-2011 - A code system for Monte Carlo simulation of electron and photon transport”, Proc. Workshop NEA/NSC/DOC(2011)5, 2011.
- [42] J. Baró, M. Roteta, J. M. Fernandez-Varea, and F. Salvat, “Analytical cross sections for Monte Carlo simulation of photon transport”, *Radiat. Phys. Chem.*, vol. 44, no. 5, pp. 531-552, 1994.
- [43] “GEANT Detector Description and Simulation Tool”, CERN Program Library Long W5013, 1995.
- [44] R. L. Ford and W. R. Nelson, “The EGS code system: computer programs for the Monte Carlo simulation of electromagnetic cascade showers (version 3)”, SLAC-210 Report, Stanford, CA, 1978.
- [45] J. Apostolakis, S. Giani, M. Maire, P. Nieminen, M.G. Pia, L. Urban, “Geant4 low energy electromagnetic models for electrons and photons” *INFN/AE-99/18*, Frascati, 1999.
- [46] S. Chauvie, G. Depaola, V. Ivanchenko, F. Longo, P. Nieminen and M. G. Pia, “Geant4 Low Energy Electromagnetic Physics”, in *Proc. Computing in High Energy and Nuclear Physics*, Beijing, China, pp. 337-340, 2001.
- [47] S. Chauvie et al., “Geant4 Low Energy Electromagnetic Physics”, in *2004 IEEE Nucl. Sci. Symp. Conf. Rec.*, pp. 1881-1885, 2004.
- [48] F. Salvat, J.M. Fernandez-Varea, E. Acosta, and J. Sempau, “Penelope - A code system for Monte Carlo simulation of electron and photon transport”, Proc. Workshop NEA, 2001.
- [49] S. Brennan and P. L. Cowan, “A suite of programs for calculating xray absorption, reflection, and diffraction performance for a variety of materials at arbitrary wavelengths”, *Rev. Sci. Instrum.*, vol., 63, pp. 850-853, 1992.
- [50] W. H. McMaster, N. Kerr Del Grande, J. H. Mallet and J. H. Hubbell, “Compilation of X-ray cross sections”, Section II Revision 1., Lawrence Livermore National Laboratory Report UCRL-50174, 1969.
- [51] A. Alexandrescu, “Modern C++ Design”, Ed.: Addison-Wesley, 2001.
- [52] S. Chauvie et al., “Geant4 physics processes for microdosimetry simulation: design foundation and implementation of the first set of models”, *IEEE Trans. Nucl. Sci.*, vol. 54, no. 6, pp. 2619-2628, 2007.
- [53] R. Y. Rubinstein and D. P. Kroese, “Simulation and the Monte Carlo Method”, 2nd ed., Wiley, Hoboken, NJ, 2008.
- [54] M. Augelli et al., “Research in Geant4 electromagnetic physics design, and its effects on computational performance and quality assurance”, in *2009 IEEE Nucl. Sci. Symp. Conf. Rec.*, pp. 177-180, 2009.
- [55] M. G. Pia et al., “Design and performance evaluations of generic programming techniques in a R&D prototype of Geant4 physics”, *J. Phys.: Conf. Ser.*, vol. 219, pp. 042019, 2010.
- [56] M. Mitchell, Engauge Digitizer [Online]. Available: <http://digitizer.sourceforge.net>.
- [57] A. Wald and J. Wolfowitz, “An exact test for randomness in the non-parametric case, based on serial correlation,” *Ann. Math. Stat.*, vol. 14, pp. 378-388, 1943.
- [58] L. W. Alvarez, F. S. Crawford, and M. L. Stevenson, “Elastic scattering of 1.6 MeV gamma rays from H, Li, C, and Al nuclei”, *Phys. Rev.*, vol. 112, no. 4, pp. 1267-1273, 1958.
- [59] S. Anand, M. Singh, and B. S. Sood, “Large angle Rayleigh scattering of 662 keV gamma rays”, *Curr. Sci.*, vol. 32, no. 9, pp. 401-402, 1963.
- [60] S. Anand and B. S. Sood, “Measurement of Z dependence of elastic scattering cross section of gamma rays”, *Nucl. Phys.*, vol. 73, no. 2, pp. 368-378, 1965.
- [61] J. Banaigs, P. Eberhard, L. Goldzahl, and E. Hara, “Diffusion élastique des rayons 1.12-1.17-1.33 et 2.62 MeV”, *J. Phys. Radium*, vol. 19, no. 1, pp. 70-72, 1958.
- [62] C. Baraldi, E. Casnati, A. Tartari, M. Andreis, and B. Singh, “Measurements of anomalous elastic scattering of 59.54 keV photons”, *Phys. Rev. A*, vol. 54, no. 6, pp. 4947-4953, 1996.
- [63] S. de Barros, O. Gonçalves, M. Gaspar, and J. R. Moreira, “Elastic scattering of 412, 468, and 662 keV γ rays”, *Phys. Rev. C*, vol. 22, no. 1, pp. 332-336, 1980.
- [64] S. de Barros, J. Eichler, M. Gaspar, and O. Gonçalves, “Rayleigh scattering of 468 keV photons by different atoms”, *Phys. Rev. C*, vol. 24, no. 4, pp. 1765-1768, 1981.
- [65] S. de Barros, J. Eichler, O. Gonçalves, and M. Gaspar, “Experiments on Rayleigh scattering of 145 keV and 317 keV photons”, *Z. Naturforsch. A*, vol. 36, pp. 595-599, 1981.
- [66] G. Basavaraju, P. Kane, L. Kissel, and R. Pratt, “Elastic scattering of 81 keV γ rays by aluminium, nickel, tantalum, gold and lead”, *Pramana*, vol. 44, pp. 545-553, 1995.
- [67] G. Basavaraju, P. Kane, and K. Varier. “Elastic scattering of 1.17 and 1.33 MeV gamma rays by molybdenum, tantalum and lead”, *Pramana*, vol. 12, pp. 665-678, 1979.
- [68] G. Basavaraju and P. P. Kane, “Elastic scattering of 1.12 MeV and 1.33 MeV γ -rays through 90° and 124.5° by different elements and the real parts of the Delbrück scattering amplitudes”, *Nucl. Phys. A*, vol. 149, no. 1, pp. 49-62, 1970.
- [69] G. Basavaraju, P. P. Kane, L. D. Kissel, and R. H. Pratt, “Elastic

- scattering of 81 keV γ rays”, *Phys. Rev. A*, vol. 49, no. 5, pp. 3664-3672, 1994.
- [70] G. Basavaraju, P. P. Kane, S. M. Lad, L. Kissel, and R. H. Pratt, “Elastic scattering of 88.03 keV γ rays”, *Phys. Rev. A*, vol. 51, no. 3, pp. 2608-2610, 1995.
- [71] A. M. Bernstein and A. K. Mann, “Scattering of gamma rays by a static electric field”, *Phys. Rev.*, vol. 110, no. 4, pp. 805-814, 1958.
- [72] D. A. Bradley, C. S. Chong, A. A. Tajuddin, A. Shukri, and A. M. Ghose, “Small-angle coherent gamma-ray scattering at 662 keV for Pb and Sn”, *Nucl. Instr. Meth. A*, vol. 280, no. 2-3, pp. 207-211, 1989.
- [73] D. A. Bradley, C. S. Chong, A. A. Tajuddin, A. Shukri, and A. M. Ghose, “Small-angle coherent γ -ray scattering for moderate- to high-atomic-number elements”, *Phys. Rev. A*, vol. 41, no. 11, pp. 5974-5979, 1990.
- [74] D. A. Bradley and A. M. Ghose, “Total-atom differential coherent-scattering cross-section measurements on Sn and Pb using moderate-energy γ rays”, *Phys. Rev. A*, vol. 33, no. 1, pp. 191-204, 1986.
- [75] C. Bui and M. Milazzo, “Measurements of anomalous dispersion in Rayleigh scattering of characteristic X-ray fluorescence”, *Nuovo Cim. D*, vol. 11, pp. 655-686, 1989.
- [76] E. Casnati, C. Baraldi, and A. Tartari, “Measurements of the total atomic differential cross section of elastic scattering of 59.54 keV photons”, *Phys. Rev. A*, vol. 42, no. 5, pp. 2627-2633, 1990.
- [77] B. K. Chatterjee and S. C. Roy, “Tables of elastic scattering cross sections of photons in the energy range 50-1500 keV for all elements in the range $13 \leq Z \leq 104$ ”, *J. Phys. Chem. Ref. Data*, vol. 27, no. 6, pp. 1011-1215, 1998.
- [78] W. Chitwattanagorn, S. Kwaengsobha, J. Jarasrangsichol, K. Rachdawanpong, and P. Oungmanee, “Elastic scattering of ^{152}Eu γ rays by various targets”, *Nucl. Instr. Meth. A*, vol. 255, no. 1-2, pp. 75-77, 1987.
- [79] W. Chitwattanagorn, R. B. Taylor, P. Teansomprasong, and I. B. Whittingham, “Elastic scattering of ^{152}Eu γ rays by Pb”, *J. Phys. G*, vol. 6, no. 9, pp. 1147-1165, 1980.
- [80] C. S. Chong, A. A. Tajuddin, A. Shukri, and D. A. Bradley, “Photon-atom scattering of 26.4 and 59.5 keV gamma rays in Mo, Nb and Zr”, *Radiat. Phys. Chem.*, vol. 47, no. 5, pp. 689-690, 1996.
- [81] N. Cindro and K. Ilakovac, “Elastic scattering of gamma-rays”, *Nucl. Phys.*, vol. 5, pp. 647-652, 1958.
- [82] W. R. Dixon and R. S. Storey, “The elastic scattering of ^{60}Co γ rays from lead”, *Can. J. Phys.*, vol. 46, no. 10, pp. 1153-1161, 1968.
- [83] J. Eichler and S. de Barros, “Coherent scattering of 59.54 keV γ rays by Al, Cu, Zn, Cd, and Pb”, *Phys. Rev. A*, vol. 32, no. 2, pp. 789-792, 1985.
- [84] J. Eichler, S. de Barros, O. Gonçalves, and M. Gaspar, “Comparison of Compton and Rayleigh scattering at 145 keV”, *Phys. Rev. A*, vol. 28, no. 6, pp. 3656-3658, 1983.
- [85] I. S. Elyaseery, A. Shukri, C. S. Chong, A. A. Tajuddin, and D. A. Bradley, “Measurement of forward scattering of 59.5 keV gamma rays by low to high Z elements”, *Radiat. Phys. Chem.*, vol. 51, no. 4-6, pp. 365-367, 1998.
- [86] I. S. Elyaseery, A. Shukri, C. S. Chong, A. A. Tajuddin, and D. A. Bradley, “Photon-atom scattering of 13.95-, 17.75-, 26.36-, and 59.54-keV photons by Cu, Zn, Zr, Nb, Mo, Ag, Cd, In, Sn, Ta, and W”, *Phys. Rev. A*, vol. 57, no. 5, pp. 3469-3477, 1998.
- [87] I. S. Elyaseery, A. Shukri, C. S. Chong, A. A. Tajuddin, and D. A. Bradley, “Total differential scattering cross-sections of 59.54 keV photons for elements in the range $29 \leq Z \leq 74$ ”, *Radiat. Phys. Chem.*, vol. 59, no. 2, pp. 211-214, 2000.
- [88] S. Erzenoğlu, L. Demir, and Y. Sahin, “Experimental studies on the coherent scattering of 59.5 keV γ -rays by Fe, Zn and Nb”, *Phys. Scr.*, vol. 56, no. 1, pp. 89, 1997.
- [89] S. Erzenoğlu, Y. Kurucu, R. Durak, and Y. Sahin, “Coherent scattering of 59.5 keV photons by Au and Pb”, *Phys. Scr.*, vol. 54, no. 2, pp. 153, 1996.
- [90] M. L. Garg, R. R. Garg, F. Hennrich, and D. Heimermann, “Elastic and inelastic scattering of photons in the X-ray energy region”, *Nucl. Instr. Meth. B*, vol. 73, no. 2, pp. 109-114, 1993.
- [91] M. Gaspar, O. Gonçalves, S. de Barros, and J. Eichler, “Some experiments on γ -scattering between 122 and 145 keV at small angles”, *Z. Phys. D*, vol. 1, pp. 287-290, 1986.
- [92] L. Goldzahl and P. Eberhard, “Contribution du champ électrique des noyaux à la diffusion élastique des γ du ^{60}Co ”, *J. Phys. Radium*, vol. 18, pp. 33-43, 1957.
- [93] O. Gonçalves, S. de Barros, M. Gaspar, A. M. Gonçalves, and J. Eichler, “Elastic scattering of 662 keV γ -rays on atoms”, *Z. Phys. D*, vol. 1, pp. 167-170, 1986.
- [94] O. D. Gonçalves and S. D. Magalhães, “Accurate Rayleigh differential cross-sections for 60 keV photons. The Ag case”, *Radiat. Phys. Chem.*, vol. 59, no. 2, pp. 201-209, 2000.
- [95] O. D. Gonçalves, H. Schechter, M. I. Lopes, and V. Chepel, “Rayleigh to Compton differential cross-section ratios in liquid xenon”, *X-Ray Spectrom.*, vol. 28, no. 5, pp. 384-387, 1999.
- [96] M. Gowda, S. J. Anasuya, and K. S. Puttaswamy, “Rayleigh scattering of 145- and 279-keV γ rays in Al, Cu, Sn, and Pb at forward angles”, *Phys. Rev. A*, vol. 33, no. 4, pp. 2301-2304, 1986.
- [97] M. L. Garg, R. R. Garg, F. Hennrich, and D. Heimermann, “Elastic and inelastic scattering of photons in the X-ray energy region”, *Nucl. Instr. Meth. B*, vol. 73, no. 2, pp. 109114, 1993.
- [98] L. P. Guy, R. B. Taylor, and I. B. Whittingham, “Small angle elastic scattering of 122 and 245 keV γ -rays”, *Nucl. Instr. Meth. B*, vol. 71, no. 4, pp. 361-365, 1992.
- [99] E. Hara, J. Banaigs, P. Eberhard, and J. Goldzahl, L. abd Mey, “Diffusion élastique par le plomb et l’étain des rayons γ de 1.33 MeV et de 1.17 MeV du ^{60}Co , et de 1.12 MeV du ^{65}Zn ”, *J. Phys. Radium*, vol. 19, pp. 668-673, 1958.
- [100] G. Hardie, J. S. DeVries, and C. Chiang, “Elastic Scattering of 1.33 MeV Photons from Lead and Uranium”, *Phys. Rev. C*, vol. 3, no. 3, pp. 1287-1293, 1971.
- [101] G. Hardie, W. J. Merrow, and D. R. Schwandt, “Large-Angle Elastic Scattering of 1.33-MeV Photons from Lead and Uranium”, *Phys. Rev. C*, vol. 1, no. 2, pp. 714-720, 1970.
- [102] U. Hauser and B. Mussnug, “Elastic scattering of 0.5 MeV gamma rays by heavy elements”, *Z. Phys. A*, vol. 195, pp. 252-272, 1966.
- [103] O. İçelli and S. Erzenoğlu, “Coherent scattering of 59.5 keV γ -rays by ^{79}Au through angles from 45° to 125° ”, *Spectrochim. Acta B*, vol. 56, no. 3, pp. 331-335, 2001.
- [104] S. Kahane, R. Moreh, and O. Shahal, “Rayleigh scattering of neutron capture γ rays from lead”, *Phys. Rev. A*, vol. 46, no. 5, pp. 2489-2494, 1992.
- [105] S. Kahane, R. Moreh, and O. Shahal, “Rayleigh scattering of $E = 465$ -2842 keV neutron capture γ -rays from Ta, In and Cu”, *Radiat. Phys. Chem.*, vol. 48, no. 4, pp. 419-426, 1996.
- [106] S. Kahane, O. Shahal, and R. Moreh, “Rayleigh scattering of neutron capture γ rays from U”, *Phys. Rev. A*, vol. 40, no. 12, pp. 6950-6957, 1989.
- [107] P. P. Kane, G. Basavaraju, S. M. Lad, K. M. Varier, L. Kissel, and R. H. Pratt, “Inelastic and anomalous elastic scattering of 88.03-keV γ rays”, *Phys. Rev. A*, vol. 36, no. 12, pp. 5626-5631, 1987.
- [108] P. P. Kane, G. Basavaraju, J. Mahajani, and A. K. Priyadarsini, “Elastic and Compton scattering of 1.17 and 1.33 MeV gamma rays through small angles”, *Nucl. Instr. Meth.*, vol. 155, no. 3, pp. 467-474, 1978.
- [109] P. P. Kane, J. Mahajani, G. Basavaraju, and A. K. Priyadarsini, “Scattering of 1.1732- and 1.3325-MeV gamma rays through small angles by carbon, aluminum, copper, tin, and lead”, *Phys. Rev. A*, vol. 28, no. 3, pp. 1509-1516, 1983.
- [110] B. Kasten, D. Schaupp, P. Rullhusen, F. Smend, M. Schumacher, and L. Kissel, “Coulomb correction effect in Delbrück scattering and atomic Rayleigh scattering of 1-4 MeV photons”, *Phys. Rev. C*, vol. 33, no. 5, pp. 1606-1615, 1986.
- [111] A. Kumar, J. S. Shahi, D. Mehta, and N. Singh, “Differential cross-section measurements for elastic scattering of 22.1 keV photons by elements with $6 \leq Z \leq 81$ ”, *Nucl. Instr. Meth. B*, vol. 194, no. 2, pp. 105-111, 2002.
- [112] A. Kumar, J. S. Shahi, M. L. Garg, S. Puri, D. Mehta, and N. Singh, “Large-angle elastic scattering of 88.03 keV photons by elements with $30 \leq Z \leq 92$ ”, *Nucl. Instr. Meth. B*, vol. 183, no. 3-4, pp. 178-188, 2001.
- [113] S. Kumar, V. Sharma, J. S. Shahi, D. Mehta, and N. Singh, “Elastic scattering of 59.54-keV γ -rays in elements with $22 \leq Z \leq 92$ at momentum transfer $0.4 \leq x \leq 4.7 \text{ \AA}^{-1}$ ”, *Eur. Phys. J. D*, vol. 55, pp. 23-33, 2009.
- [114] J. P. Lestone, R. B. Taylor, P. Teansomprasong, and I. B. Whittingham, “Elastic scattering of ^{152}Eu and ^{154}Eu γ rays by atoms”, *Phys. Rev. A*, vol. 37, no. 9, pp. 3218-3231, 1988.
- [115] A. C. Mandal, D. Mitra, M. Sarkar, and D. Bhattacharya, “Differential elastic scattering cross sections of 22.1 keV x ray by elements in the range $22 \leq Z \leq 82$ ”, *Phys. Rev. A*, vol. 66, no. 4, pp. 042705, 2002.
- [116] A. K. Mann, “Elastic scattering of gamma rays”, *Phys. Rev.*, vol. 101, no. 1, pp. 4-8, 1956.
- [117] S. Messelt and A. Storruste, “Elastic scattering of gamma rays”, *Proc. Phys. Soc. A*, vol. 69, no. 5, pp. 381-387, 1956.

- [118] W. Muckenheim and M. Schumacher, "Delbrück and Rayleigh scattering by uranium investigated at photon energies between 0.1 and 1.5 MeV", *J. Phys. G*, vol. 6, no. 10, pp. 1237-1251, 1980.
- [119] V. A. N. Murty, V. Lakshminarayana, and S. Jnanananda, "Elastic scattering of 1.12 MeV gamma rays", *Nucl. Phys.*, vol. 62, no. 2, pp. 296-304, 1965.
- [120] V. A. N. Murty, V. Lakshminarayana, and S. Jnanananda, "The elastic scattering of 662 keV gamma rays", *Proc. Phys. Soc.*, vol. 85, no. 6, pp. 1075-1081, 1965.
- [121] S. S. Nandi, S. K. Ghose, S. K. Sen Gupta, and N. Chaudhuri, "Study of anomalous dispersion in elastic scattering of 59.5 keV photons at K-absorption edges of target atoms", *J. Phys. B*, vol. 22, no. 8, pp. 1175-1182, 1989.
- [122] A. Nath and A. M. Ghose, "Measurement of coherent scattering cross sections of gamma rays at small angles", *Nucl. Phys.*, vol. 57, pp. 547-564, 1964.
- [123] N. G. Nayak, K. M. Balakrishna, and K. Siddappa, "Experimental study on coherent scattering of 145.4 and 279.2 keV gamma rays by medium and heavy elements", *J. Phys. B*, vol. 26, no. 22, pp. 4117-4127, 1993.
- [124] N. G. Nayak, K. Siddappa, K. M. Balakrishna, and N. Lingappa, "Coherent scattering of 59.5 keV γ rays by some medium and heavy elements", *Phys. Rev. A*, vol. 45, no. 7, pp. 4490-4493, 1992.
- [125] M. S. Prasad, G. K. Raju, K. N. Murty, V. A. N. Murty, and V. Lakshminarayana, "Elastic-scattering of 279 keV gamma-rays", *Indian J. Pure Appl. Phys.*, vol. 16, no. 9, pp. 836-840, 1978.
- [126] M. S. Prasad, G. K. Raju, K. N. Murty, V. A. N. Murty, and V. Lakshminarayana, "Elastic scattering of 145 keV gamma rays", *J. Phys. B*, vol. 11, no. 23, pp. 3969-3976, 1978.
- [127] S. Puri, B. Chand, D. Mehta, M. L. Garg, N. Singh, and P. N. Trehan, "Differential cross section measurements for the elastic scattering of 59.5 keV photons by elements in the atomic region $13 \leq Z \leq 82$ ", *Nucl. Instr. Meth. B*, vol. 111, no. 3-4, pp. 209-214, 1996.
- [128] R. Quivy, "Mesure absolue de la section efficace différentielle de diffusion cohérente des gamma de 662 keV dans le plomb", *Nucl. Phys. A*, vol. 101, no. 2, pp. 417-423, 1967.
- [129] N. Ramanathan, T. J. Kennett, and W. V. Prestwich, "An experimental investigation of small angle photon elastic scattering", *Can. J. Phys.*, vol. 57, no. 3, pp. 343-352, 1979.
- [130] D. V. Rao, "Measurements of whole-atom coherent and incoherent scattering cross-sections in some rare earth elements at low photon energies", *Appl. Radiat. Isot.*, vol. 42, no. 9, pp. 855-859, 1991.
- [131] D. V. Rao, R. Cesareo, A. Brunetti, and G. E. Gigante, "Influence of solid state environment effects on measured elastic scattering cross sections in the X-ray regime and the associated anomalous dispersion", *Phys. Scr.*, vol. 62, no. 1, pp. 81-87, 2000.
- [132] D. V. Rao, R. Cesareo, and G. E. Gigante, "Coherent and incoherent scattering of 14.93, 17.44 and 21.12 keV photons from Al, Cu, Sr, Cd, Ce, Pr, Sm, Pt, Au and Pb", *Phys. Scr.*, vol. 50, no. 3, pp. 314-320, 1994.
- [133] D. V. Rao, R. Cesareo, and G. E. Gigante, "Elastic and Compton scattering cross sections in the atomic region $12 \leq Z \leq 82$ ", *Appl. Radiat. Isot.*, vol. 47, no. 2, pp. 219-227, 1996.
- [134] D. V. Rao, R. Cesareo, and G. E. Gigante, "Rayleigh and Compton scattering cross sections for low, medium and high Z elements in the energy region $23.18 \leq E \leq 30.85$ keV", *Phys. Scr.*, vol. 54, no. 4, pp. 362-367, 1996.
- [135] D. V. Rao, R. Cesareo, and G. E. Gigante, "Elastic and Compton scattering of X-ray photons from platinum in the momentum transfer region $1.3175 \text{ h } \text{Å}^{-1} \leq q \leq 2.0448 \text{ h } \text{Å}^{-1}$ ", *Phys. Scr.*, vol. 55, no. 3, pp. 305-309, 1997.
- [136] D. V. Rao, R. Cesareo, and G. E. Gigante, "Elastic scattering and the associated anomalous dispersion in the vicinity of Cd, In, Sn and Sb, K-absorption edges", *Appl. Radiat. Isot.*, vol. 48, no. 6, pp. 789-806, 1997.
- [137] D. V. Rao, R. Cesareo, and G. E. Gigante, "A new method to estimate elastic scattering cross sections in the X-ray region and the associated anomalous dispersion", *Appl. Radiat. Isot.*, vol. 49, no. 7, pp. 835-844, 1998.
- [138] D. V. Rao, R. Cesareo, and G. E. Gigante, "Elastic scattering and the associated anomalous dispersion in the energy range $8.63 \leq E \leq 42.75$ keV from heavy atoms", *X-Ray Spectrom.*, vol. 27, no. 6, pp. 381-389, 1998.
- [139] D. V. Rao and G. E. Gigante, "Coherent and incoherent scattering of low-energy X-ray photons in the atomic region $13 \leq Z \leq 82$ ", *Can. J. Phys.*, vol. 74, no. 1-2, pp. 10-16, 1996.
- [140] D. V. Rao, G. E. Gigante, and R. Cesareo, "Coherent and incoherent scattering of 42.75 and 47.24 keV x-ray photons scattered from Al, Cu, Y, Mo, Au and Pb", *X-Ray Spectrom.*, vol. 24, no. 4, pp. 172-176, 1995.
- [141] S.C. Roy, A. Nath, and A. M. Ghose, "Measurement of coherent scattering cross-sections of gamma rays at very low momentum transfer", *Nucl. Instr. Meth.*, vol. 131, pp. 163-166, 1975.
- [142] H. Schopper, "Die elastische streuung von γ -Strahlen bei kleinen streuwinkeln", *Z. Phys. A*, vol. 147, pp. 253-260, 1957.
- [143] M. Schumacher, "Elastic scattering of 145-, 279-, 412-, and 662-keV γ rays from lead", *Phys. Rev.*, vol. 182, no. 1, pp. 7-14, 1969.
- [144] M. Schumacher, F. Smend, and I. Borchert, "Elastic scattering of γ -rays from lead for energies from 0.145 to 1.33 MeV", *Nucl. Phys. A*, vol. 206, no. 3, pp. 531-544, 1973.
- [145] M. Schumacher and A. Stoffregen, "Rayleigh scattering of 59.54 keV photons from Zn, Mo, Sn, Ta, Au and Pb through angles from 60° to 150° ", *Z. Phys. A*, vol. 283, pp. 15-19, 1977.
- [146] S. K. Sen Gupta, N. C. Paul, Bose J., G. C. Goswami, Das S. C., and N. Chaudhuri, "Atomic Rayleigh scattering of phonons in the vicinity of K-absorption edges", *J. Phys. B*, vol. 15, no. 4, pp. 595-602, 1982.
- [147] S. K. Sen Gupta, N. C. Paul, S. C. Roy, and N. Chaudhuri, "New measurements of coherent and incoherent photon scattering by low, medium and high Z atoms", *J. Phys. B*, vol. 12, no. 7, pp. 1211-1224, 1979.
- [148] J. S. Shahi, S. Puri, D. Mehta, M. L. Garg, N. Singh, and P. N. Trehan, "Elastic scattering of 22.1 keV photons by elements in the atomic region $12 \leq Z \leq 92$ ", *Phys. Rev. A*, vol. 55, no. 5, pp. 3557-3565, 1997.
- [149] J. S. Shahi, S. Puri, D. Mehta, M. L. Garg, N. Singh, and P. N. Trehan, "Large-angle elastic scattering of 59.54 keV photons by elements with $12 \leq Z \leq 92$ ", *Phys. Rev. A*, vol. 57, no. 6, pp. 4327-4334, 1998.
- [150] K. Siddappa, N. G. Nayak, K. M. Balakrishna, and N. Lingappa, "Experimental studies on atomic form factors at $4.808\text{-}\text{Å}^{-1}$ photon momentum transfer", *Phys. Rev. A*, vol. 39, no. 10, pp. 5106-5110, 1989.
- [151] F. Smend and H. Czerwinski, "Large-angle elastic scattering of 59.54 keV photons by Kr and Xe", *Z. Phys. D*, vol. 1, pp. 139-140, 1986.
- [152] F. Smend, M. Schumacher, and I. Borchert, "The Z-dependence of the elastic scattering of γ -rays", *Nucl. Phys. A*, vol. 213, no. 2, pp. 309-316, 1973.
- [153] K. G. Standing and J. V. Jovanovich, "The elastic scattering of Co 60 γ -rays", *Can. J. Phys.*, vol. 40, no. 5, pp. 622-653, 1962.
- [154] R. B. Taylor, P. Teansomprasong, and I. B. Whittingham, "Elastic scattering of ^{152}Eu γ rays by tungsten", *Aust. J. Phys.*, vol. 34, pp. 125-133, 1981.
- [155] R. B. Taylor, P. Teansomprasong, and I. B. Whittingham, "Elastic scattering of ^{152}Eu and ^{154}Eu γ -rays", *Nucl. Instr. Meth. A*, vol. 255, no. 1-2, pp. 68-74, 1987.
- [156] K. M. Varier and M. P. Unnikrishnan, "Elastic and inelastic scattering of 59.54 keV gamma rays", *Nucl. Instr. Meth. A*, vol. 280, no. 2-3, pp. 428-432, 1989.
- [157] W. M. J. Veigele, "Photon cross sections from 0.1 keV to 1 MeV for elements $Z = 1$ to $Z = 94$ ", *Atom. Data Nucl. Data Tables*, vol. 5, no. 1, pp. 51-111, 1973.
- [158] R. R. Wilson, "Scattering of 1.33 MeV gamma-rays by an electric field", *Phys. Rev.*, vol. 90, no. 4, pp. 720-721, 1953.
- [159] C. Gowda, T. K. Umesh, and R. Gowda, "A simple method to measure the total coherent scattering cross sections of elements", *Nucl. Instr. Meth. B*, vol. 95, pp. 127-130, 1995.
- [160] C. Gowda and R. Gowda, "Studies on coherent scattering below 1 MeV", Thesis, Univ. of Mysore, 1994, Online. Available: <http://dspace.vidyanidhi.org.in:8080/dspace/handle/2009/1328>.
- [161] IEEE Computer Society, "IEEE Standard for Software Verification and Validation", IEEE Std 1012-2004, Jun. 2005.
- [162] ISO/IEC, "International Standard, Information Technology Software Life Cycle Process, ISO 12207", 2008-2011.
- [163] G. A. P. Cirrone et al., "A Goodness-of-Fit Statistical Toolkit", *IEEE Trans. Nucl. Sci.*, vol. 51, no. 5, pp. 2056-2063, 2004.
- [164] B. Mascialino, A. Pfeiffer, M. G. Pia, A. Ribon, and P. Viarengo, "New developments of the Goodness-of-Fit Statistical Toolkit", *IEEE Trans. Nucl. Sci.*, vol. 53, no. 6, pp. 3834-3841, 2006.
- [165] R. K. Bock and W. Krischer, "The Data Analysis BriefBook", Ed. Springer, Berlin, 1998.
- [166] A. N. Kolmogorov, "Sulla determinazione empirica di una legge di distribuzione", *Gior. Ist. Ital. Attuari*, vol. 4, pp. 83-91, 1933.
- [167] N. V. Smirnov, "On the estimation of the discrepancy between empirical curves of distributions for two independent samples", *Bull. Math. Univ. Moscou*, 1939.

- [168] T. W. Anderson and D. A. Darling, "Asymptotic theory of certain goodness of fit criteria based on stochastic processes", *Anls. Ma. St.*, vol. 23, pp. 193-212, 1952.
- [169] T. W. Anderson and D. A. Darling, "A test of goodness of fit", *JASA*, vol. 49, pp. 765-769, 1954.
- [170] H. Cramér, "On the composition of elementary errors. Second paper: statistical applications", *Skand. Aktuarietidskr.*, vol. 11, pp. 13-74, pp. 141-180, 1928.
- [171] R. von Mises, "Wahrscheinlichkeitsrechnung und ihre Anwendung in der Statistik und theoretischen Physik", Leipzig: F. Duticke, 1931.
- [172] R. A. Fisher, "On the interpretation of χ^2 from contingency tables, and the calculation of P", *J. Royal Stat. Soc.*, vol. 85, no. 1, pp. 87-94, 1922.
- [173] F. Yates, "Contingency table involving small numbers and the χ^2 test", *J. Royal Stat. Soc. Suppl.*, vol. 1, pp. 217-235, 1934.
- [174] K. Pearson, "On the χ^2 test of Goodness of Fit", *Biometrika*, vol. 14, no. 1-2, pp. 186-191, 1922.
- [175] R. Barlow, "Statistics A guide to the use of statistical methods in the physical sciences", Ed: John Wiley & Sons, 1989.
- [176] S. C. Roy, L. Kissel and R. H. Pratt, "Elastic photon scattering at small momentum transfer and validity of form-factor theories", *Phys. Rev. A*, vol. 27, pp. 285-290, 1983.
- [177] T. V. George, L. Goldstein, L. Slama, and M. Yokoyama, "Scattering of Ruby-Laser Beam by Gases", *Phys. Rev.* 137, pp. A369-A380, 1965.
- [178] R. R. Rudder and D. R. Bach, "Rayleigh Scattering of Ruby-Laser Light by Neutral Gases" *J. Opt. Soc. Am.*, vol. 58, pp. 1260-1266, 1968.
- [179] S. J. Buckman, J. W. T. Cooper, M. T. Elford, M. Inokuti, Y. Itikawa, and H. Tawara, "Interactions of Photons and Electrons with Atoms", Springer-Verlag, 2000.
- [180] Shardanand and Y. Mikawa, "Photon Scattering Cross Sections at Lyman- α (1215.7 Å) for He and Ne", *J. Quant. Spectrosc. Radiat. Transfer*, vol. 7, pp. 605-609, 1967.
- [181] Shardanand and A. D. P. Rao, "Absolute Rayleigh scattering cross sections of gases and freons of stratospheric interest in the visible and ultraviolet regions", NASA Technical Note TN D-8442, Washington DC, 1977.
- [182] P. Gill and D. W. O. Heddle, "Determination of the Refractive Indices of Gases in the Vacuum Ultraviolet. II The Rayleigh Scattering Method", *J. Opt. Soc. Am.*, vol. 53, pp. 847-851, 1963.
- [183] P. D. Chopra and D. W. O. Heddle, "Polarization free measurements of Rayleigh scattering of Lyman α ", *J. Phys. B*, vol. 7, no. 17, 2421-2428, 1974.
- [184] J. P. Geindre, J. C. Gauthier and J. F. Delpéch, "Rayleigh Light Scattering with a Low Power He-Ne Laser", *Phys. Lett. A*, vol. 44, pp. 149-150, 1973.
- [185] D. E. Gray, "American Institute of Physics Handbook", Third Edition, McGraw-Hill, pp. 6-110, 1972.
- [186] Allen, C. W., "Astrophysical Quantities" Third Edition, The Athlone Press, University of London, p. 92, 1973.
- [187] D. W. O. Heddle, R. E. Jennings and A. S. L. Parsons, "Determination of the refractive indices of gases in the vacuum ultraviolet. I. The Cerenkov radiation method", *J. Opt. Soc. Am.*, vol. 53, pp. 840-846, 1963.
- [188] G. I. Chashchina, V. C. Gladushchak and E. Y. Shreider, "Determination of the Refractive Index of Argon and the Oscillator Strength of Its Resonance Lines", *Opt. Spectrosc.*, vol. 24, pp. 542-543, 1968.
- [189] R. B. Cairns, F. F. Marmo and J. A. R. Samson, "Photon Scattering by Argon in the Vacuum Ultraviolet", *J. Opt. Soc. Am.*, vol. 60, pp. 211-213, 1970.
- [190] M. Snee and W. Ubachs, "Direct measurement of the Rayleigh scattering cross section in various gases", *J. Quant. Spectrosc. Radiat. Transfer*, vol. 92, pp. 293-310, 2005.
- [191] M. Han, C. H. Kim, L. Moneta, M.G. Pia, H. Seo, "Physics data management tools: computational evolutions and benchmarks" in *Proc. Joint In. Conf. on Supercomputing Nucl. Appl. and Monte Carlo*, p. 10269, 2010.
- [192] M. Han, M. G. Pia, H. Seo, L. Moneta, and C. H. Kim, "Physics data management tools for Monte Carlo transport: Computational evolutions and benchmarks", in *IEEE Nucl. Sci. Symp. Conf. Rec.*, pp. 95-101, 2010.
- [193] M. Han et al., "New data libraries and physics data management tools", *J. Phys. Conf. Ser.*, vol. 331, p. 042010, 2011.